AD-A192 288 CALCULATION OF THE BREN JAPANESE HOUSE SHIELDING EXPERIMENTS(U) SCIENCE APPLICATIONS INTERNATIONAL CORP SAN DIEGO CA W A WOOLSON ET AL 22 AUG 83 SAIC-83-1020 1/1

UNCLASSIFIED DNA-TR-81-308 DNA001-81-C-0206 F/G 18/6 NL

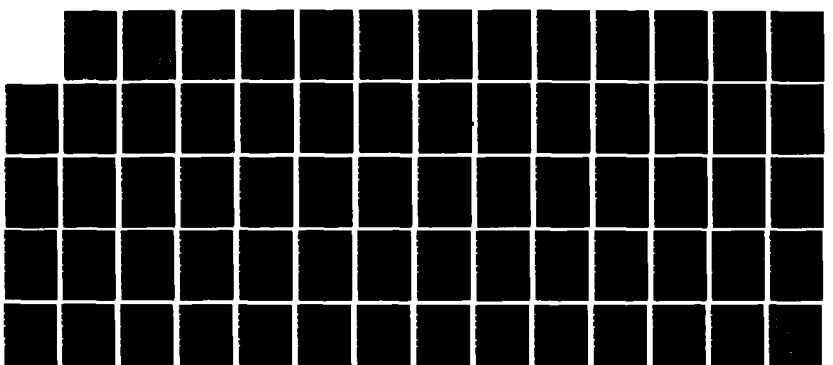

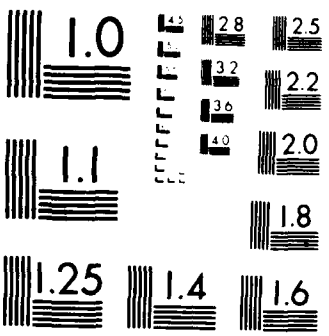
1.0
1.1
1.25
1.4
1.6
1.8
2.0
2.2
2.5
2.8
3.2
3.6
4.0

AD-A192 288

DNA-TR-81-308

CALCULATION OF THE BREN JAPANESE HOUSE SHIELDING EXPERIMENTS

W. A. Woolson
M. L. Gritzner
Science Applications International Corp.
10260 Campus Point Drive
San Diego, CA 92121

22 August 1983

Technical Report

CONTRACT No. DNA 001-81-C-0206

THIS WORK WAS SPONSORED BY THE DEFENSE NUCLEAR AGENCY
UNDER RDT&E RMSS CODE X350083469 U99QMXK000067 H2590D.

Prepared for
Director
DEFENSE NUCLEAR AGENCY
Washington, DC 20305-1000

Destroy this report when it is no longer needed. Do not return to sender.

PLEASE NOTIFY THE DEFENSE NUCLEAR AGENCY ATTN: TITL, WASHINGTON, DC 20305 1000, IF YOUR ADDRESS IS INCORRECT, IF YOU WISH IT DELETED FROM THE DISTRIBUTION LIST, OR IF THE ADDRESSEE IS NO LONGER EMPLOYED BY YOUR ORGANIZATION.

DISTRIBUTION LIST UPDATE

This mailer is provided to enable DNA to maintain current distribution lists for reports. We would appreciate your providing the requested information.

☐ Add the individual listed to your distribution list.

☐ Delete the cited organization/individual.

☐ Change of address.

NAME: _____

ORGANIZATION: _____

OLD ADDRESS	CURRENT ADDRESS
_____	_____
_____	_____
_____	_____

TELEPHONE NUMBER: ( ) _____

SUBJECT AREA(s) OF INTEREST:

_____	_____
_____	_____
_____	_____

DNA OR OTHER GOVERNMENT CONTRACT NUMBER: _____

CERTIFICATION OF NEED-TO-KNOW BY GOVERNMENT SPONSOR (if other than DNA):

SPONSORING ORGANIZATION: _____

CONTRACTING OFFICER OR REPRESENTATIVE: _____

SIGNATURE: _____

CUT HERE AND RETURN

REPORT DOCUMENTATION PAGE

1a REPORT SECURITY CLASSIFICATION UNCLASSIFIED	1b RESTRICTIVE MARKINGS
2a SECURITY CLASSIFICATION AUTHORITY N/A since Unclassified	3 DISTRIBUTION/AVAILABILITY OF REPORT Approved for public release; distribution is unlimited.
2b DECLASSIFICATION/DOWNGRADING SCHEDULE N/A since Unclassified	
4 PERFORMING ORGANIZATION REPORT NUMBER(S) SAI-83-1020	5 MONITORING ORGANIZATION REPORT NUMBER(S) DNA-TR-81-308
6a NAME OF PERFORMING ORGANIZATION Science Applications International Corp. 6b OFFICE SYMBOL (If applicable)	7a NAME OF MONITORING ORGANIZATION Director Defense Nuclear Agency
6c ADDRESS (City, State, and ZIP Code) 10260 Campus Point Drive San Diego, CA 92121	7b ADDRESS (City, State, and ZIP Code) Washington, DC 20305-1000
8a NAME OF FUNDING/SPONSORING ORGANIZATION 8b OFFICE SYMBOL (If applicable) STBE/Campbell	9 PROCUREMENT INSTRUMENT IDENTIFICATION NUMBER DNA 001-81-C-0206
8c ADDRESS (City, State, and ZIP Code)	10 SOURCE OF FUNDING NUMBERS PROGRAM ELEMENT NO: 62715H; PROJECT NO: U99QMX; TASK NO: K0; WORK UNIT ACCESSION NO: DH005549

11 TITLE (Include Security Classification)

CALCULATION OF THE BREN JAPANESE HOUSE SHIELDING EXPERIMENTS

12 PERSONAL AUTHOR(S)
Woolson, William A. and Gritzner, Michael L.

13a TYPE OF REPORT	13b TIME COVERED	14 DATE OF REPORT (Year, Month, Day)	15 PAGE COUNT
Technical	FROM 821001 TO 830501	830822	66

16 SUPPLEMENTARY NOTATION
This work was sponsored by the Defense Nuclear Agency under RDT&E RMSS Code X350083469 U99QMXK000067 H2590D.

17 COSATI CODES			18 SUBJECT TERMS (Continue on reverse if necessary and identify by block number)
FIELD	GROUP	SUB-GROUP	
6	7		Nuclear Radiation, Neutron, Discrete Ordinates
18	3		Protection Factor, Gamma Ray, Adjoint Transport
			Transmission, Monte Carlo, House Shielding

19 ABSTRACT (Continue on reverse if necessary and identify by block number)

The techniques used to calculate the house shielding as part of the dosimetry reassessment for survivors of the Hiroshima and Nagasaki A-bombs are validated by modeling the Operation BREN Japanese house shielding experiments and comparing calculated radiation transmission factors to the measured values. Single and two-story houses were modeled, as well as multiple house configurations. In all cases, the agreement for the ^{60}Co transmission and the reactor neutron transmission was excellent with most cases better than 10 percent. The agreement for the reactor gamma-ray transmission was poor; analysis indicates the discrepancy is probably due to problems in the measurements. The calculational procedure consists of performing a surface integral of the incident energy-angular fluence in air-over-ground geometries from the source with the energy-angular importance of the detector response in the three-dimensional house configuration. The air-over-ground fluence is computed by discrete ordinates; the importance function is computed by Monte Carlo in the adjoint

20 DISTRIBUTION/AVAILABILITY OF ABSTRACT	21 ABSTRACT SECURITY CLASSIFICATION
☐ UNCLASSIFIED/UNLIMITED ☒ SAME AS RPT ☐ DTIC USERS	UNCLASSIFIED
22a NAME OF RESPONSIBLE INDIVIDUAL Sandra E. Young	22b TELEPHONE (Include Area Code) (202)325-7042
	22c OFFICE SYMBOL DNA/CSTI

DD FORM 1473, 84 MAR 83 APR edition may be used until exhausted
All other editions are obsolete

18. SUBJECT TERMS (Continued)

BREN

19. ABSTRACT (Continued)

mode. The excellent agreement obtained between the calculations and measurements for the ^{60}Co source and reactor neutrons demonstrates that the calculational procedure can provide accurate house transmission factors required in the dosimetry estimates for over half of the A-bomb survivor subjects used in radiobiological effects studies.

CONVERSION TABLE

Conversion factors for U.S. Customary to metric (SI) units of measurement

MULTIPLY TO GET	BY	TO GET DIVIDE
angstrom	1.000 000 X E -10	meters (m)
atmosphere (normal)	1.013 25 X E +2	kilo pascal (kPa)
bar	1.000 000 X E +2	kilo pascal (kPa)
barn	1.000 000 X E -28	meter^2 (m^2)
British thermal unit (thermochemical)	1.054 350 X E +3	joule (J)
calorie (thermochemical)	4.184 000	joule (J)
cal (thermochemical)/cm^2	4.184 000 X E -2	mega joule/m^2 (MJ/m^2)
curie	3.700 000 X E +1	*giga becquerel (GBq)
degree (angle)	1.745 329 X E -2	radian (rad)
degree Fahrenheit	$t_k = (t°f + 459.67)/1.8$	degree kelvin (K)
electron volt	1.602 19 X E -19	joule (J)
erg	1.000 000 X E -7	joule (J)
erg/second	1.000 000 X E -7	watt (W)
foot	3.048 000 X E -1	meter (m)
foot-pound-force	1.355 818	joule (J)
gallon (U.S. liquid)	3.785 412 X E -3	meter^3 (m^3)
inch	2.540 000 X E -2	meter (m)
jerk	1.000 000 X E +9	joule (J)
joule/kilogram (J/kg) (radiation dose absorbed)	1.000 000	Gray (Gy)
kilotons	4.183	terajoules
kip (1000 lbf)	4.448 222 X E +3	newton (N)
kip/inch^2 (ksi)	6.894 757 X E +3	kilo pascal (kPa)
ktap	1.000 000 X E +2	newton-second/m^2 ($N-s/m^2$)
micron	1.000 000 X E -6	meter (m)
mil	2.540 000 X E -5	meter (m)
mile (international)	1.609 344 X E +3	meter (m)
ounce	2.834 952 X E -2	kilogram (kg)
pound-force (lbs avoirdupois)	4.448 222	newton (N)
pound-force inch	1.129 848 X E -1	newton-meter (N·m)
pound-force/inch	1.751 268 X E +2	newton/meter (N/m)
pound-force/foot^2	4.788 026 X E -2	kilo pascal (kPa)
pound-force/inch^2 (psi)	6.894 757	kilo pascal (kPa)
pound-mass (lbm avoirdupois)	4.535 924 X E -1	kilogram (kg)
pound-mass-foot^2 (moment of inertia)	4.214 011 X E -2	kilogram-meter^2 ($kg·m^2$)
pound-mass/foot^3	1.601 846 X E +1	kilogram/meter^3 (kg/m^3)
rad (radiation dose absorbed)	1.000 000 X E -2	**Gray (Gy)
roentgen	2.579 760 X E -4	coulomb/kilogram (C/kg)
shake	1.000 000 X E -8	second (s)
slug	1.459 390 X E +1	kilogram (kg)
torr (mm Hg, 0° C)	1.333 22 X E -1	kilo pascal (kPa)

*The becquerel (Bq) is the SI unit of radioactivity; 1 Bq = 1 event/s
**The Gray (Gy) is the SI unit of absorbed radiation

TABLE OF CONTENTS

LIST OF ILLUSTRATIONS

LIST OF TABLES

SECTION 1

INTRODUCTION

Several American and Japanese institutions are engaged in research efforts to produce and validate a revised dosimetry system for radiobiological analysis of the survivors of the Hiroshima and Nagasaki A-bombs.[1,2] The revised system will be produced by modern calculational techniques as distinguished from the dosimetry system presently used (called T65D) which relied mainly on Nevada Nuclear Weapons Tests and the BREN (Bare Reactor Experiment Nevada) experiments.[3] In situ data, the Nevada Weapon tests, the BREN experiments, and other appropriate experimental data are being used to validate the techniques and computer codes used for calculations of the weapon-produced radiation sources, the air-over-ground radiation transport, the house shielding, and the in-body radiation transport.[1]

Work on calculating the free-in-air (FIA) radiation environment is well advanced with detailed two-dimensional calculations of the radiation output of the asymmetric LITTLE BOY device exploded over Hiroshima completed by Whalen[2] and with subsequent calculations of the prompt radiation environment by Pace and the delayed radiation by Scott.[2] An independent calculation of the FIA environment at both Hiroshima and Nagasaki from older, one-dimensional weapon output radiation computations by Preeg[4] for the A-bombs has been reported by Loewe.[5]

The FIA radiation environment can be significantly perturbed by the house occupied by the survivor and by nearby neighboring houses. Compared to the FIA environment, the exposure environment at the survivor location may be reduced by factors from two to four, be shifted in energy and have a reduced neutron to gamma-ray ratio. We are engaged in a program to calculate the

house shielding effects on the exposure radiation environment and to incorporate these effects into the revised dosimetry system.

As a first step in this research effort, we have validated our method by calculating the BREN house transmission experiments[6] which were used to derive the house shielding for the T65D system. Although we believe that the T65D house radiation transmission factors are in error and need revision,[7] the BREN experiments can be used to validate the calculational procedures. The same techniques can be used to determine transmission factors with more realistic models of the A-bomb events than could be achieved in experiments such as BREN. This paper presents our work to compare calculated house transmission factors with reported measured data from the BREN experiments.

SECTION 2
BACKGROUND

Detailed descriptions of the location and position at the time of bomb detonation (ATB) of the A-bomb survivors in the Radiation Effects Research Foundation (RERF) data bases, such as Life Span Study (LSS),[8] have been compiled from interviews and placed in shielding files. Nine categories were used to describe the shielding situation of the survivor. The number of subjects in each category for the proximally exposed group (less than 1600-m ground range at Hiroshima and less than 2000-m at Nagasaki) is given in Table 1. Over half of the survivors in the data base were inside residential houses ATB.

In the T65D system, the perturbation of the FIA radiation by residential houses was estimated by transmission factors for neutrons and gamma rays which multiplied the FIA kermas to give the exposure neutron and gamma-ray kerma.[3] Later, organ dose factors were developed to account for body shielding.[9] The transmission factors for individual survivors were calculated by a parametric model called the "Nine Parameter Formula" (NPF) based on a regression analysis of the BREN house transmission experiments.[6] The nine parameters were derived for individual survivors from examination of his/her shielding file and coded for computer access.[10]

The BREN house transmission experiments consisted of exposing radiation analogs of Japanese residential houses to radiation from the bare Health Physics Research Reactor (HPRR) and a ^{60}Co source.[6] The sources were suspended up to 1125 feet from a tower and the houses were placed at ground ranges from 750 to 1200 yards from the tower.[a] The transmission factors reported were the ratio of the neutron and gamma-rays kermas measured inside

[a] In the following, we will use the dimensional specifications (inches, feet, yards) appearing in the BREN experiment reports for clarity and ease of comparison.

Table 1. Distribution of shielding cases in proximally exposed group.

Category	Percentage		
	Combined	Hiroshima	Nagasaki
1. Open - Unshielded	7.3	8.1	5.6
2. Open - Partial Shielded	3.8	2.3	6.6
3. Open - Terrain	4.5	0.2	12.9
4. Open - Building Shielded	8.2	10.3	4.2
5. Concrete Building	3.5	1.6	7.2
6. Japanese House	51.8	58.3	39.3
7. Factory Building	4.3	0.2	12.5
8. Air Raid Shelter	1.4	0.2	3.9
9. Miscellaneous	0.3	0.2	0.4
Unknown	14.8	18.7	7.5
TOTAL CASES	18,770	12,375	6,395

the houses at various locations to kermas measured at the same ground range at locations free from local obstructions. The neutron measurements were made with a recoil proton proportional counter and the gamma-ray measurements were performed with Geiger-Mueller tubes.

With this experimental procedure, the gamma-ray kerma measured inside the house includes gamma rays produced by neutron inelastic and capture reactions with the house materials. Thus, the gamma-ray transmission factors are dependent on the local neutron environment. For the nominal configuration at BREN (HPRR at 1125 ft height, houses at 750 yds) the calculated neutron to gamma-ray kerma ratio is nearly three, while at Hiroshima and Nagasaki the same ratio is less than 0.1 and 0.01, respectively, at ground ranges where survivors in the data bases were present (beyond about 900 m). This problem was first examined by Marcum who concluded that the gamma-ray transmission factors used in T65D based on BREN data were too high by a factor of 1.6[7,11] because of the higher house gamma ray contribution.

Although the BREN experiments did not accurately replicate the radiation environments at Hiroshima and Nagasaki, they are valuable experiments for validating calculational procedures which can then be applied to the Japanese house shielding problem. Our method to calculate the house shielding uses the Monte Carlo technique in the adjoint mode to compute the energy-angular radiation response of the house cluster surrounding the detector location. This response function can then be coupled to the FIA energy-angular environment to estimate the exposure environment.

SECTION 3

THEORY

The radiation environment inside a small structure far removed from a source of radiation can be determined by partitioning the problem into separate transport calculations that are then coupled to provide the overall solution. This partition consists of a calculation of the global radiation environment in simplified geometry coupled to an appropriate radiation transport calculation in a detailed geometry model of the structure. The first calculation is a discrete ordinates numerical solution to the Boltzmann transport equation (BTE) in two-dimensional air over flat ground geometry; the latter calculation is often a Monte Carlo solution to the adjoint BTE in a three-dimensional model of the structure.

The theoretical basis for this solution technique is the fact that the radiation environment inside a volume enclosed by a non-reentrant surface can be completely characterized by the knowledge of the incoming particle flux at the surface and the radiation sources within the volume. Since the structures here have no internal sources of radiation, we can determine the interior radiation environment if we know the incoming particle flux on a non-reentrant surface, e.g., sphere or cylinder enclosing the structure.

The theory for this procedure has been rigorously developed and adequately explained by many authors, notably Hoffmann, et al.[12] We provide here only a summary to maintain continuity for the reader. Following Hoffman, the rigorous solution to the complete problem (including both source and structure geometry) is given by

$$H\phi(\overline{P}) = S(\overline{P}) \qquad (1)$$

where H is the Boltzmann operator; $\phi(\overline{P})$ is the flux in six-dimensional phase space denoted by $\overline{P}$; and $S(\overline{P})$ is the source. The result of interest λ (i.e., some observable quantity) involves integration of a known flux response function $R(\overline{P})$ with the particle flux,

$$\lambda = \int \phi(\overline{P}) R(\overline{P}) d\overline{P} \quad . \tag{2}$$

Now, we assume that the source $S(\overline{P})$ is zero in the region of the structure and the response function $R(\overline{P})$ is zero outside the region of the structure. Let $\overline{r}_s$ denote the vector of the locus of points describing a nonreentrant surface enclosing volume $\overline{v}$ containing the structure. Let $\overline{P}_v$ denote phase space elements in $\overline{v}$. We require

$$S(\overline{P}_v) = 0 \tag{3}$$

and

$$R(\overline{P}) = 0, \quad \overline{P} \notin \overline{P}_v \quad . \tag{4}$$

In this case, the rigorous solution for the flux in $\overline{v}$ can be written as

$$H\phi(\overline{P}_v) = -(\overline{n}\cdot\overline{\Omega})\phi(\overline{P}_v)\delta(\overline{r}-\overline{r}_s) \; ; \; \overline{n}\cdot\overline{\Omega} < 0, \tag{5}$$

where $\overline{n}$ is the outward directed normal to the non-reentrant surface, and the spatial and angular elements of $\overline{P}$ are denoted by $\overline{r}$ and $\overline{\Omega}$, respectively. We have replaced Eq. (1) for the flux in $\overline{v}$ by an equivalent expression with Eq. (5).

The well-known property of the Boltzmann operator

$$\int_{\overline{V}} \phi^*(\overline{P}_V) H\phi(\overline{P}_V) d\overline{P}_V = \int_{\overline{V}} \phi(\overline{P}_V) H^*\phi^*(\overline{P}_V) d\overline{P}_V + \int_{\overline{V}} (\overline{n}\cdot\overline{\Omega})\phi(\overline{P}_V)\phi^*(\overline{P}_V)\delta(\overline{r}-\overline{r}_s) d\overline{P}_V \qquad (6)$$

reduces to

$$\lambda = \int_{\overline{V}} \phi(\overline{P}_V) R(\overline{R}_V) d\overline{P}_V = - \int_{\overline{V}} (\overline{n}\cdot\overline{\Omega})\phi(\overline{P}_V)\phi^*(\overline{P}_V)\delta(\overline{r}-\overline{r}_s) d\overline{P}_V \qquad (7)$$

by noting that the LHS of Eq. (6) is zero since $H\phi(\overline{P}_V) = S(\overline{P}_V) \equiv 0$ and by substituting

$$H^*\phi^*(\overline{P}_V) = R(\overline{P}_V) \quad . \qquad (8)$$

Here, H* is the adjoint Boltzmann operator. By virtue of Eq. (5), the result, λ, cannot depend on the outward directed flux on the surface of $\overline{V}$. This suggests the boundary condition for the solution for $\phi^*(\overline{P}_V)$ as

$$(\overline{n}\cdot\overline{\Omega})\phi^*(\overline{P}_V)\delta(\overline{r}-\overline{r}_s) = 0, \ \overline{n}\cdot\overline{\Omega} \geq 0 \qquad (9)$$

Thus, by solving Eq. (8) for $\phi^*(\overline{P}_V)$ with boundary condition given by Eq. (9) (vacuum boundary), the result, λ, can be obtained via

$$\lambda = -\int (\bar{n}\cdot\bar{\Omega})\phi(\bar{P}_v)\phi^*(\bar{P}_v)\delta(\bar{r}-\bar{r}_s)d\bar{P}_v, \quad \bar{n}\cdot\bar{\Omega} < 0 \tag{10}$$

from Eq. (7).

Our solution, at this point, has no approximations. But the flux $\phi(\bar{P}_v)$ in Eq. (10) contains the structure in the problem. We now solve for a new flux

$$H_a\phi_a(\bar{P}) = S(\bar{P}) \tag{11}$$

for the same source but in a simpler, approximate geometry without the details of the structure present, as embodied in the operator H_a. We then form the approximate result

$$\lambda_a = -\int (\bar{n}\cdot\bar{\Omega})\phi_a(\bar{P}_v)\phi^*(\bar{P}_v)\delta(\bar{r}-\bar{r}_s)d\bar{P}_v, \quad \bar{n}\cdot\bar{\Omega} < 0, \tag{12}$$

with an error

$$\varepsilon = -\int (\bar{n}\cdot\bar{\Omega})(\phi_a(\bar{P}_v) - \phi(\bar{P}_v))\phi^*(\bar{P}_v)\delta(\bar{r}-\bar{r}_s)d\bar{P}_v, \quad \bar{n}\cdot\bar{\Omega} < 0. \tag{13}$$

Note that $\phi^*(\bar{P}_v)$ is still the rigorous solution in $\bar{P}_v$.

To summarize, we calculate the effect of interest inside a complex structure in air-over-ground geometry by performing a surface integral of the adjoint flux computed in the complex geometry with the incoming surface flux from the source computed in a simplified geometry. The error of this approximate approach is directly associated with the difference in the incoming flux at the surface between the simplified geometry and the complex geometry.

Thus, assuming an accurate adjoint solution $\phi^*(\bar{P}_v)$ can be obtained, assuming the incoming flux on the surface surrounding the structure is not significantly perturbed by its presence, and assuming the calculation of the flux, $\phi_a(\bar{P}_v)$, in the simplified geometry model is accurate; the solution given by Eq. (12) should be a reasonable estimate of the desired result in Eq. (2).

SECTION 4
APPLICATION OF THE THEORY

A code system called VCS (Vehicle Code System)[13] was developed to calculate $\phi^*(\bar{P}_v)\delta(\bar{r}-\bar{r}_s)$ and perform the numerical intergration of Eq. (12) with the forward fluxes, $\phi_a(\bar{P}_v)$, from a calculation with the two-dimensional discrete ordinates code, DOT.[14] This code system was originally designed to calculate radiation protection factors for military vehicles such as tanks and armored personnel carriers. We have adapted the VCS code with some major and minor modifications for the house shielding analyses. In the following, we discuss how our modified VCS code system is used to estimate the radiation environments in structures.

The calculation of the forward flux, $\phi_a(\bar{P}_v)$, is performed with the DOT code. The DOT code uses multigroup, multitable cross sections coupling neutron transport, gamma-ray production from inelastic and capture reactions, and gamma-ray transport. The method utilizes discrete ordinates in two-dimensional geometries (spherical, cylindrical, and slab). The cylindrical geometry is used for VCS calculations consisting of air over a flat ground plane with the source located above the ground on the axis of symmetry. This simplified two material geometry is adequate for calculations of the BREN reactor and ^{60}Co source suspended above the desert in Nevada; however, calculations for built-up areas such as Hiroshima and Nagasaki may require a mush model of buildings to account for the distal effects of the built-up urban areas on localized radiation environments.

The DOT code for cylindrical geometry provides a computer file of the angular flux quantity

$$\phi_a(z,r,\eta,\psi,E)$$

where the spatial coordinates (z,r) and angular coordinates (η,ψ) are defined in Figure 1. Note that η refers to the cosine of angle of the angular direction with the z axis and ψ is the angle of the projection in the x-y plane with respect to the radial vector. (The subscript "a" for approximate is retained to note that the calculation does not include the specific structure in which the radiation environment is desired.) The flux is provided for discrete mesh intervals in z,r space, in η,ψ angular space, and for energy groups in E. Let ω_{ij} be the fraction of 4π angular space ascribed to the discrete ordinate (η_i,ψ_{ij}). The scalar flux can be calculated as

$$\phi_a(z,r,E) = \sum_i \sum_j \phi_a(z,r,\eta_i,\psi_{ij},E)\omega_{ij} \quad . \tag{14}$$

The units on the angular flux from DOT are particles per cm^2 per fraction of 4π space. The VISA code of VCS is used to access the DOT angular flux file and retrieve only flux values near the air/ground interface required for the coupling calculation of Eq. (12).

The adjoint quantity, $\phi^*(\overline{P}_v)\delta(\overline{r}-\overline{r}_s)$, is computed with an adaptation of the MORSE Monte Carlo code[15] called MORSE/VCS. The MORSE code uses multigroup, multitable cross sections and operates in both the forward and adjoint modes. Special user routines can be written and interfaced with MORSE to handle source specifications and flux estimation. Transport calculations can be carried out in complex geometrical configurations modeled with the combinatorial geometry package in MORSE.

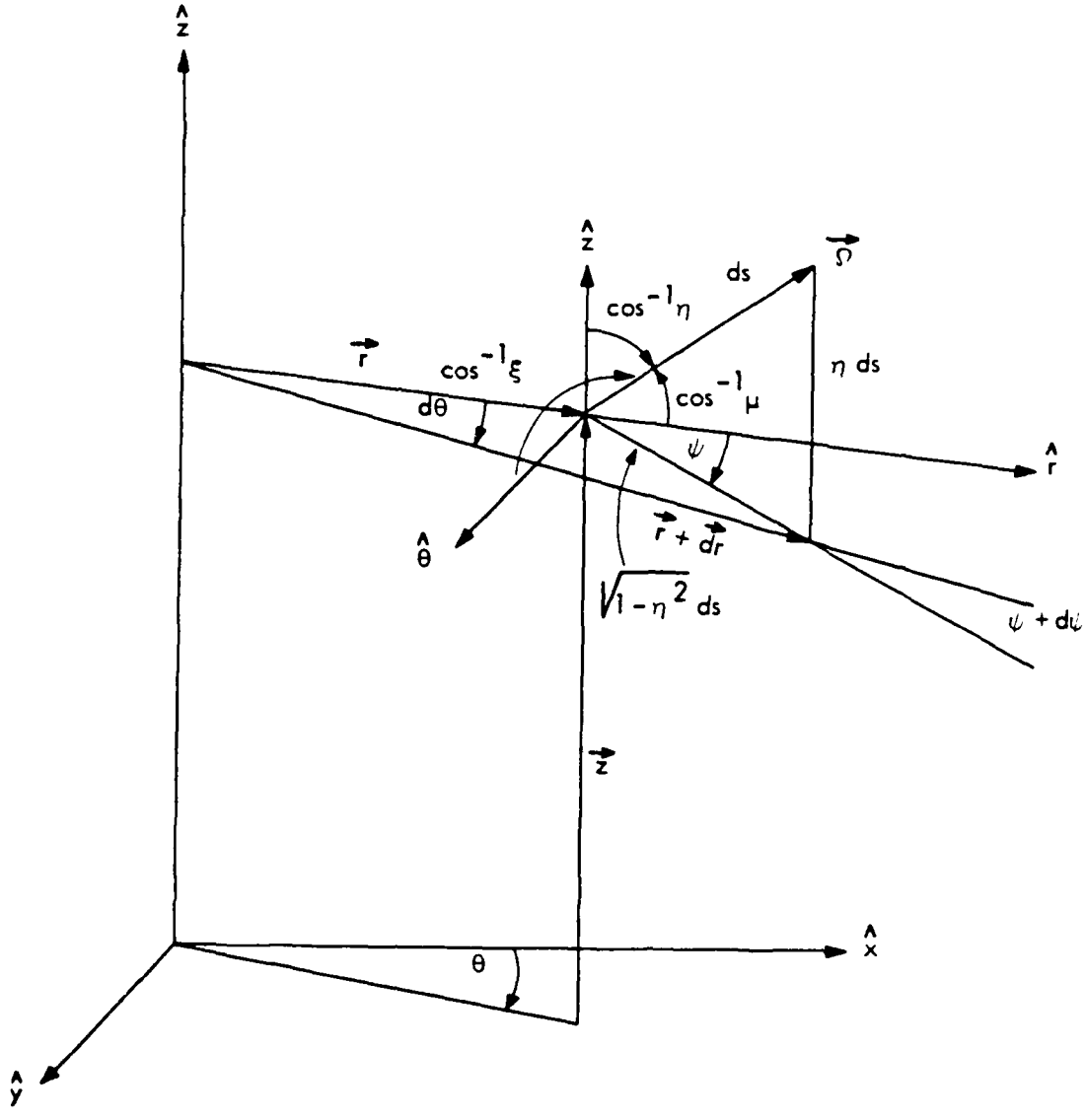

Figure 1. The coordinate system for cylindrical geometry.

The primary modification to MORSE in the MORSE/VCS code is the inclusion in the code of routines to write a particle leakage file containing the source energy group, the leakage energy group, the leakage direction cosines, and the "z" coordinate (height above the ground plane). A particle "leaks" in the adjoint MORSE/VCS calculation when it crosses the vacuum boundary surface that defines the volume including the structure, in accordance with the boundary condition specified in Eq. (9). This volume is a right circular cylinder with the axis normal to the ground. The cylinder entirely encloses the object of interest and extends a few tens of centimeters into the ground.

Minor modifications that have been made for these house shielding calculations include the provision to write on the leakage file the entire source and leakage phase space parameters. This will enable eventual coupling to man phantom calculations to estimate body shielding. The geometrical surface (e.g., roof, right side window, etc.) that the particle crossed when escaping into the surrounding air or ground is also written for later interpretation of the results.

The major modification to the code was the inclusion of adjoint in-group biasing developed by Scott[16] to improve the statistical precision of adjoint coupled calculations where gamma rays become thermal neutrons, and then the thermal neutrons upscatter to higher energies. If these calculations are performed in the standard manner, large variations in particle weights occur (hence, large standard deviations in results) becuase the adjoint thermal neutrons are "forced" to upscatter with a large fair game weight correction.

The adjoint calculation is performed with a detailed mathematical model of the structure using the combinatorial geometry package available with MORSE. The model contains the ground and air surrounding the structure inside the leakage surfaces of the cylinder. The adjoint simulation commences at the detector location in the structure. As the adjoint particle interacts with the materials in the building, air and/or ground, it gains energy and gamma rays produce adjoint secondary neutrons. The selection of scattered energy and angle uses the same procedures and routines as the forward calculational procedure, except the reaction cross sections for adjoint calculations are inverted from the forward set. When a particle leaks from the system, the relevant parameters are written to the leakage file and a new history is started.

When the calculation is completed, this leakage file contains the individual statistical weights of all the leaking particles as a function of source and leakage variables. This may be written as

$$W(\bar{R}_L, \bar{\Omega}_L, \bar{E}_L, \bar{R}_s, \bar{\Omega}_s, \bar{E}_s)$$

where W is the statistical weight of the particle, $(\bar{R}_L, \bar{\Omega}_L, E_L)$ and $(\bar{R}_s, \bar{\Omega}_s, E_s)$ are leakage and source position, angle, and energy phase space parameters, respectively. In the following we also employ the notation

$$\bar{R}_L = (x_L, y_L, z_L) \tag{15}$$

to decompose the spatial vector into individual orthogonal components.

The DRC code of VCS reads the DOT forward flux tape prepared by VISA and the adjoint leakage file provided by MORSE/VCS, and then performs the numerical integration of Eq. (12).

Because the structure, in principle, can be oriented in any direction with respect to the source, the angular coordinates of each leakage particle are transformed to the desired orientation. This transformation with a matrix derived from Eulerian angle rotation is given by

$$\overline{\Omega}'_L = \overline{\overline{T}} \cdot \overline{\Omega}_L \tag{16}$$

$$\overline{\Omega}'_s = \overline{\overline{T}} \cdot \overline{\Omega}_s \tag{17}$$

where $\overline{\overline{T}}$ is the transformation matrix. The standard VCS code only permits rotation of the structure about an axis parallel to the Z direction. We have added the generalized rotation to examine effects of small "tilts" in the structure, even though the ground planes of the DOT and adjoint calculations would not precisely align.

With the transformed angle coordinates, the angular bin of the DOT quadrature containing the leakage direction is found. First, the "eta" level is determined based on the value

$$\eta = \hat{z} \cdot \overline{\Omega}'_L \quad , \tag{18}$$

where $\hat{z}$ is the unit vector normal to the ground plane. The relative weight (or fraction of 4π space) associated with each polar eta level is calculated by DRC via

$$\omega_i = \sum_j \omega_{ij} \tag{19}$$

and "i" index (eta level) is found such that

$$\sum_{i'=1}^{i-1} \omega_{i'} \leq \frac{1}{2}(\eta + 1) < \sum_{i'=1}^{i} \omega_{i'}. \tag{20}$$

The phi level ("j" index) is based on the value:

$$\cos \psi_j = \hat{r} \cdot \bar{\Omega}'_L \cdot (1 - \eta_i^2)^{1/2} \tag{21}$$

(where $\hat{r}$ is the unit vector in the radial direction) and is found via

$$\frac{1}{\omega_i} \sum_{j'=1}^{j-1} \omega_{ij'} \leq \frac{1}{2}(\cos \psi_j + 1) < \frac{1}{\omega_i} \sum_{j'=1}^{j} \omega_{ij'} \quad . \tag{22}$$

This procedure determines the discrete ordinate $\Omega_{ij} = (\eta_i, \psi_{ij})$ for the DOT angular flux.

The estimate of exposure flux by Eq. (12) is then given by

$$\phi(r_s, \bar{\Omega}'_s, E_s) = \langle \phi_a(z_L, r_s, \Omega_{ij}, E_L) \cdot W(\bar{R}_L, \bar{\Omega}'_L, E_L, \bar{R}_s, \bar{\Omega}'_s, E_s) \rangle \tag{23}$$

where r_s the ground range of the in-structure detector from the source in the DOT calculation and where the brackets $\langle\rangle$ indicate the average over the leakage variables for all histories. Note that this estimate only depends on the "z" spatial coordinate of the adjoint leakage. The forward DOT flux for the coupling is only defined at the radius of the detector location r_s. This assumes that the variation in flux with radius is small compared to the radial extent of the structure.

By preserving the full phase space parameters of the adjoint source, the full energy angular distribution of the exposure flux can be calculated. This can be used for detailed calculations of radiation transport in man phantoms using the same surface integral technique (Eq. 12) with an additional adjoint calculation in the man phantom starting at the organ location. This facility to "nest" calculations using successive adjoint calculations was incorporated by us into the standard version of VCS. This is done by defining the angular flux in the same angle bins as the DOT quadrature, so that the flux calculated from a coupling procedure is in the same format as the VISA processed DOT angular flux.

The exposure flux inside the structure can be used to calculate detector responses and kermas via

$$\lambda(r_s) = \int \phi(r_s, \bar{\Omega}'_s, E_s) R(E_s) d\bar{\Omega}'_s dE_s \qquad (24)$$

where $R(E_s)$ is the energy-dependent response. Note that if the energy angular dependent response is known, it can be integrated with the angular dependence of the exposure flux.

In addition to the approximation introduced by the theory, the practical application with the VCS methodology introduces approximations and sources of uncertainty. There exist the usual sources of uncertainty associated with any calculational technique, including the knowledge of the physical variables associated with configuration (e.g., the air density, construction materials, structure layout); the basic data input to the calculation, such as nuclear cross sections; and modeling of the configuration and the

physics data (e.g., number of geometry regions, energy group structure, quadrature order).

There are also sources of uncertainty peculiar to the surface integral coupling method. One of the most important is the coupling to DOT fluxes at a single radial point corresponding to the ground range of the detector. Although VCS performs the surface integral as a function of a z coordinate, the code assumes the flux does not vary in the radial direction across the leakage surface. To analyze this assumption, we write the radial variation of the flux approximately as

$$\phi(r) \propto \frac{e^{-r/L}}{r^2} \tag{25}$$

for some appropriate relaxation length, L. This is a good representation over a limited range at least and was used, for example, in the T65D system to provide the doses at all ground ranges used by RERF. For small Δr, we can write

$$\frac{\phi(r) - \phi(r+\Delta r)}{\phi(r)} \sim \Delta r \left(\frac{1}{L} + \frac{2}{r}\right) \quad . \tag{26}$$

The relaxation length is on the order of 300 m for many sources in air-over-ground and choosing r to be the same, we estimate as a near worst case (since r is usually larger), that the flux changes by 10% in 10 m. This indicates that the assumption is reasonable for small structures; however, the method may have to be modified for problems involving a cluster of houses for which there may be unacceptable variation in the flux across the larger volume enclosed by the leakage surface.

Another issue more difficult to analyze is the adequacy of the resolution of the angular flux in the DOT quadrature. The VCS procedure assumes the flux is constant within the solid angle defined by the quadrature boundaries. Furthermore, the uncollided flux is "smeared" over the most forward directed quadrature interval. The concern may be that streaming paths, such as windows, may receive too much or too little incident flux, depending on its relation to the quadrature boundaries and the "true" angular variation of the flux.

SECTION 5

COMPARISON WITH THE BREN EXPERIMENTS

5.1 BREN HOUSE TRANSMISSION MEASUREMENTS.

The Operation BREN experiments took place at the Nevada Test Site (NTS) in the spring of 1962.[17] The experiments consisted of suspending a small bare reactor and a ^{60}Co source from a tower at heights of up to 1125 feet and making measurements of free field and house perturbed neutron and gamma-ray kermas. The ratio of the kermas measured at detectors in (and around) the houses to free field kerma was reported as the house transmission factor for the detector location.

The Health Physics Research Reactor (HPRR) was used for the neutron (and secondary gamma ray) source.[18] The reactor consisted of a highly enriched uranium-molybdenum alloy metal annulus with an outside diameter of 0.203 m and inside diameter of 0.05 m. Details of the reactor configuration are found in Ref. 18. The small size of the reactor and lack of reflector provides a hard, nearly unmoderated fission spectrum of neutrons. The ^{60}Co source used at BREN contained 1200 Ci at time of manufacture which had decayed to 800 Ci at the time of the experiments.

The free field gamma-ray kermas produced by the HPRR and ^{60}Co source were measured with the "Phil" detector described by Wagner and Hurst.[19] It consists of a small Geiger-Mueller tube which was enclosed by tin and lead sheaths to provide (according to the developers) a uniform kerma per count as a function of incident gamma-ray energy from 100 keV to 10 MeV. However, at the time of the BREN experiments, the highest reported calibration energy was the ^{60}Co gamma-ray lines (1.17, 1.33 MeV). When a neutron field was present, the Phil was further enclosed by a ^{6}Li shield to reduce the neutron

response from thermal neutron capture. It was claimed that the Phil had no fast neutron response. To improve counting statistics, measurements inside the houses were performed with a larger Geiger-Mueller detector. Details of the calibration or encapsulation materials for this detector, however, were never reported in the open literature. The neutron kerma measurements were made with the RADSAN proportional counter.[20]

The houses constructed at NTS for the BREN experiments were designed to be radiation analogs of typical Japanese residential houses at Hiroshima and Nagasaki ATB.[6] Three models were built designated as House A (a typical one-story family house); House B (a larger two-story residence), and House C (a small one-story tenement house). The houses were constructed full scale to the very uniform dimensions of Japanese dwellings. In place of Japanese construction materials, however, the designers used a cement asbestos board produced by the Johns Mansville Corporation under the trade name TRANSITE, which was used in many houses in East Tennessee near the Oak Ridge National Laboratory (ORNL).[21] The use of cement asbestos board was justified by the results of direct beam radiation measurements at ORNL which showed the ratio of PuBe neutron attenuation to ^{60}Co attenuation similar to the ratio for a Japanese house wall section.[22] The exterior walls consisted of 1-inch and 3/4-inch thick sheets butted together and placed in slots on wood-framing members. The interior walls were actually thicker and consisted of two 1-inch sheets. The roof had the same total thickness as the exterior walls but was composed of two 1/2-inch sheets and a 3/4-inch sheet.

The house models were built on skids enabling them to be towed and placed into different configurations and orientations. In addition, single walls of some of the houses were built and could be moved from place to place to produce additional shielding effects.

5.2 FREE-IN-AIR ENVIORNMENT.

The VCS code system is designed to couple the adjoint calculation of building response with free-in-air environments calculated with the discrete ordinates code, DOT. Calculations with DOT of the free-field radiation environments produced by the BREN ^{60}Co source and the BREN HPRR reactor used in this study have been performed by Dolatshahi and Kaul.[23] Here we provide a summary of the comparison of their calculations with the measurements of the FIA kerma made during the BREN experiments. A comparison of the kerma computed by DOT with measurements for BREN ^{60}Co source at a height of 1125 feet is presented in Figure 2. The "r^2 kerma" as a function of slant range is presented at the air/ground interface. This comparison and at other detector heights[23] shows excellent agreement between the FIA calculations and measurements. Similar comparisons of the neutron kerma from the HPRR reactor are presented in Figure 3. The DOT calculation for the neutron kerma is in excellent agreement with measurements at all heights for all ground ranges. However, calculated gamma-ray kerma associated with the HPRR source do not agree well with experiment, as indicated in Figure 4 with the calculations consistently low by about 40%. As discussed in Ref. 23, the cause of this discrepancy is unresolved, although it is possible that the gamma-ray detectors were not properly calibrated for the high energy gamma rays from the fission products and the neutron-induced capture gamma rays. Neutron interactions with the detector system itself may also account for the high gamma-ray measurement

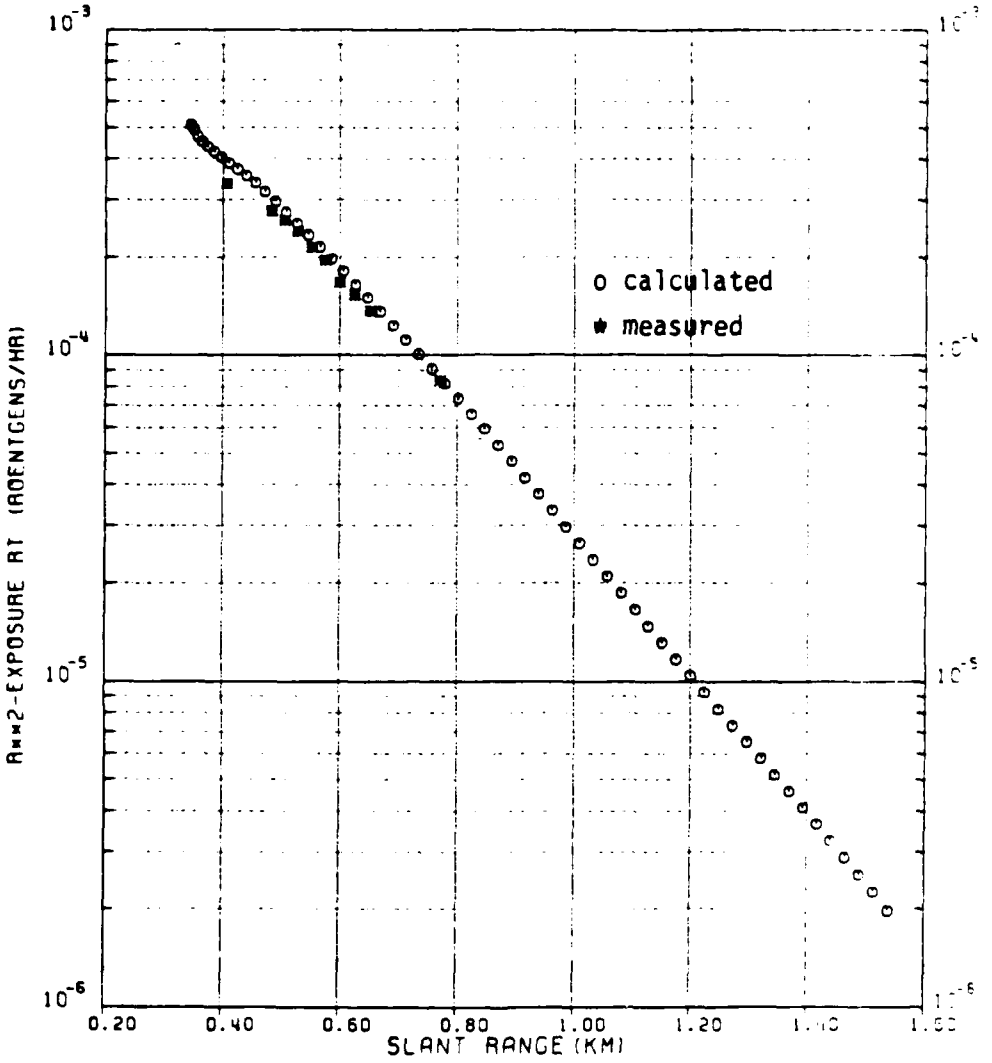

Figure 2. BREN ^{60}Co exposure rate versus slant range measured and calculated at ground surface.

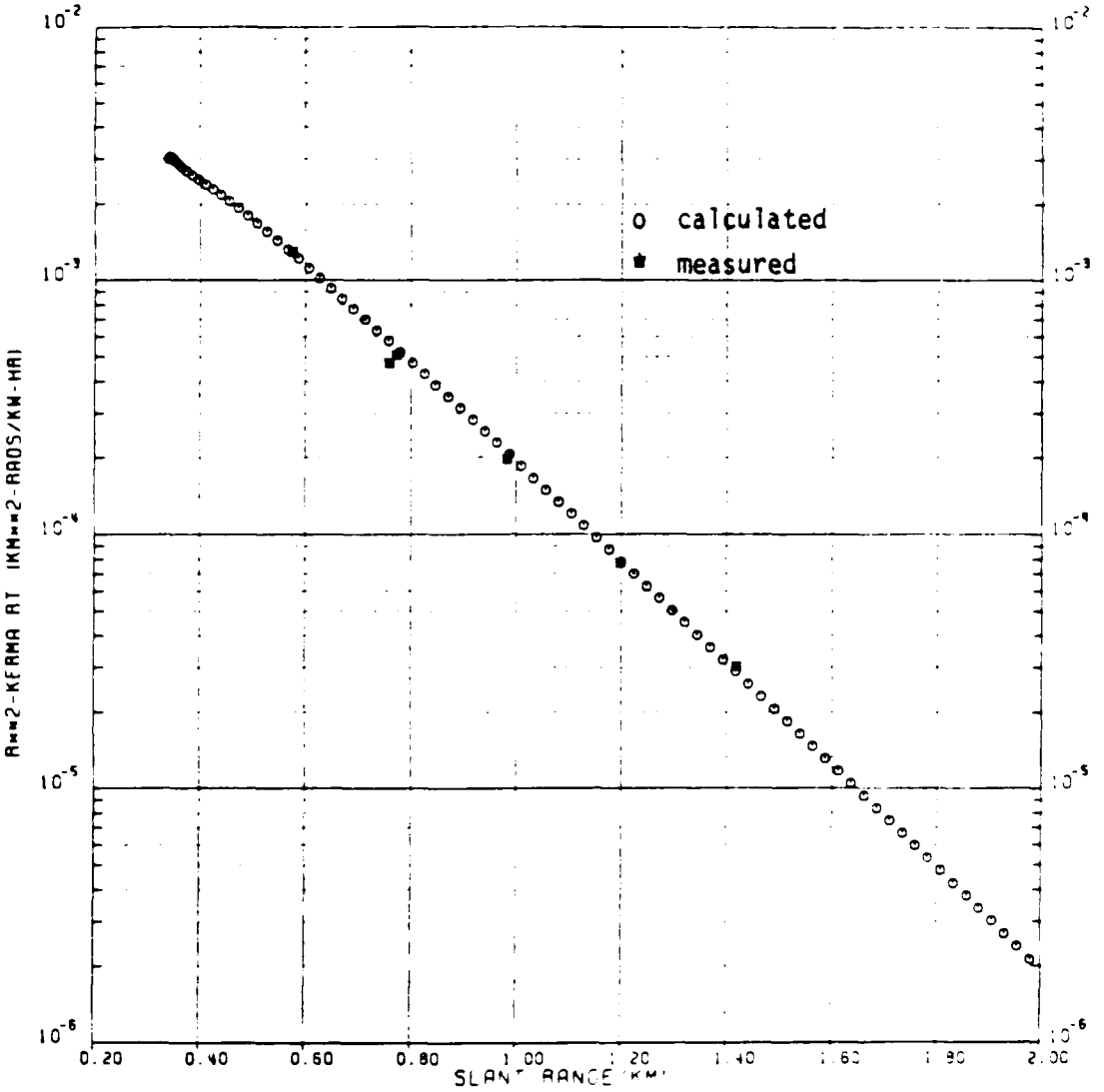

Figure 3. BREN reactor neutron kerma rate versus slant range measured and calculated at the ground surface.

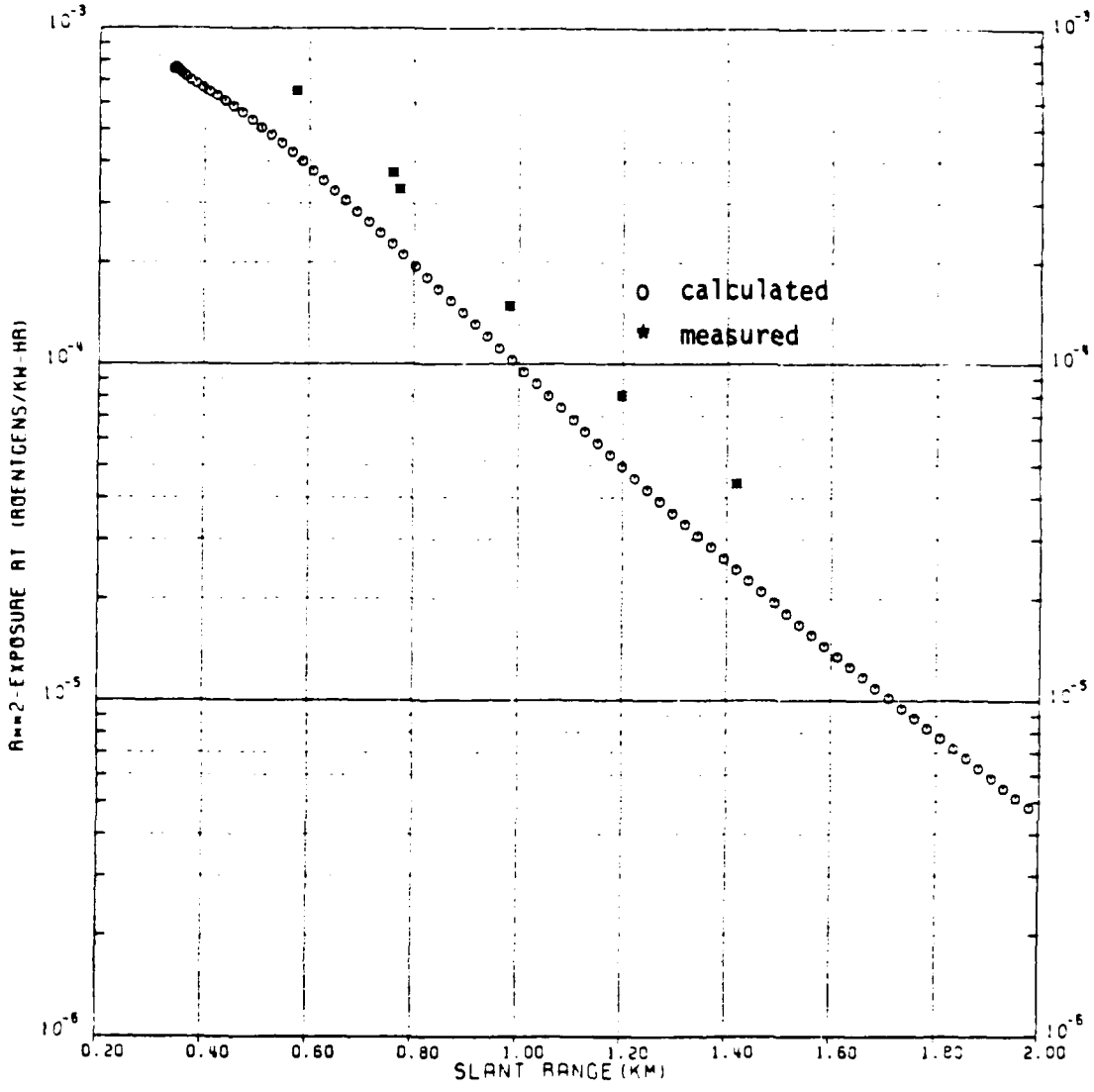

Figure 4. BREN reactor gamma-ray kerma rate versus slant range measured and calculated at the ground surface.

reported. The same calculational technique has been applied to a similar reactor operating at the Ballistic Research Laboratory in Maryland. Comparisons of calculated gamma-ray spectra with measurements made with a NE-213 detector show much better agreement than the integral kerma comparisons for BREN.[23]

All our house transmission calculations use the energy angular fluence tape produced by Dolatshahi and Kaul's DOT calculations of the BREN reactor and ^{60}Co experiments.

5.3 CALCULATIONS FOR HOUSE A.

The first set of house transmission calculations were performed for a house model identified as "House A" in the BREN experiments. House A was designed to replicate a standard, one-story, typical Japanese residential house present at both Hiroshima and Nagasaki. A computer-drawn representation of our combinatorial geometry model of House A is presented in Figure 5. The House A geometry model for the radiation transport, as well as other houses used in the calculations, is based on as-built drawings obtained from Nevada test site personnel and from dimensional measurements made in 1982 by the authors on the house frames that were still standing at the Nevada test site. Some of the dimensions for House A are indicated in the figure.

Samples of the cement asbestos board used for the house walls, partitions and roofs were obtained from the Nevada test site in the vicinity of the houses, and an elemental analysis was performed at the Oak Ridge

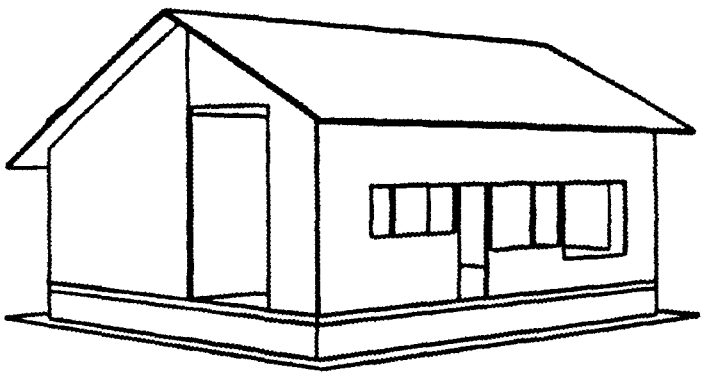

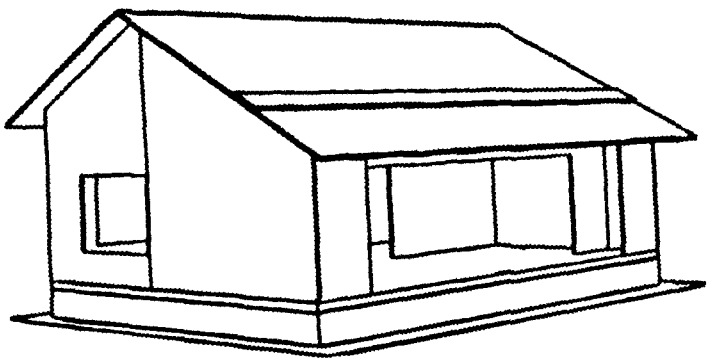

TYPICAL DIMENSIONS

Length:	28' 4"
Width:	22' 4"
Roof Peak:	13' 6"
Interior Openings Height:	5' 8"
Interior Partitions Height:	9' 2"

Figure 5. House A geometry model.

National Laboratory.[24] The result of the analysis is presented in Table 2. Calculations for the ^{60}Co source used the "PVC" cross section set[25] consisting of P_5 Legendre expansion of the scattering angular distributions and 36 multigroups for gamma-ray transport. Calculations for the HPRR source used the DLC-31[26] P_3 expanded cross sections in coupled multigroups (37 neutron group - 21 gamma-ray group). Elemental cross sections available in both libraries (indicated in Table 2) were mixed at the measured concentration to form the macroscopic cross sections for dry TRANSITE. Those elements without cross sections compose 0.04% of the mass of the composition. Our calculations employed a partial density 2.08 gm/cc of TRANSITE plus a partial density of 0.023 gm/cc of moisture. Simple geometry ^{60}Co attenuation measurements of the house material were made at our laboratory by Shreve.[27] A comparison of the attenuation measurements, with the attenuation predicted by the cross sections used in our calculations, is shown in Figure 6.

Calculations using VCS were performed for House A for several different locations and detector heights. Our calculations for House A and other configurations were not designed to be exhaustive but a representative comparison with the variety of measurements. Furthermore, we have not edited our results; every calculation that we have performed to compare with BREN experiments is presented. The detector locations are indicated in Figure 7 which presents a computer drawing of our House A model looking down from the top with no roof and showing the interior partitions and openings. The detector identification system is identical to the one used to report the BREN measurements.[6] The house was oriented so that the large opening (the veranda) faced the source. The source was located at a ground range of 750 yards and height of 1125 feet. Comparisons of the calculated and measured

Table 2. Composition of dry TRANSITE sample.*

Element	Concentration†	Available Cross Sections#	Element	Concentration†	Available Cross Sections#
H	1.43%	X	Zn	32.7	
Li	14.2	X	Ga	3.4	
Be	0.44	X	As	4.3	
B	11.8	X	Br	1.0	
C	3.73%	X	Rb	7.1	
N	0.011%	X	Sr	260	
O	50.9%	X	Y	3.88	
Na	774	X	Zr	21.7	
Mg	13.7%	X	Nb	5.2	
Al	1.06%	X	Mo	0.42	X
Si	12.8%	X	Ag	0.20	
Cl	169	X	Sb	0.18	
P	170	X	Ba	53.8	X
K	0.201%	X	La	5.3	
Ca	13.7%	X	Ce	11.1	
Sc	4.6		Sm	0.9	
Ti	542	X	Eu	0.28	
V	30.2	X	Tb	0.32	
Cr	650	X	Hf	0.93	
Mn	581	X	Ta	0.22	X
Fe	2.94%	X	W	0.20	X
Co	44.2		Pb	3.3	X
Ni	761	X	Th	1.8	X
Cu	5.05	X	U	0.69	X
			Total	100.9%	

*Dried 24 hours at 105-110°C with 1.08% moisture loss.

†Concentration in PPM by mass, except where noted as mass percent.

#Used PVC and DLC-31 Cross Section Libraries.[25,26] Elements mixed at reported concentration for dry TRANSITE. *Those elements without cross sections are 0.04% by mass of the composition*

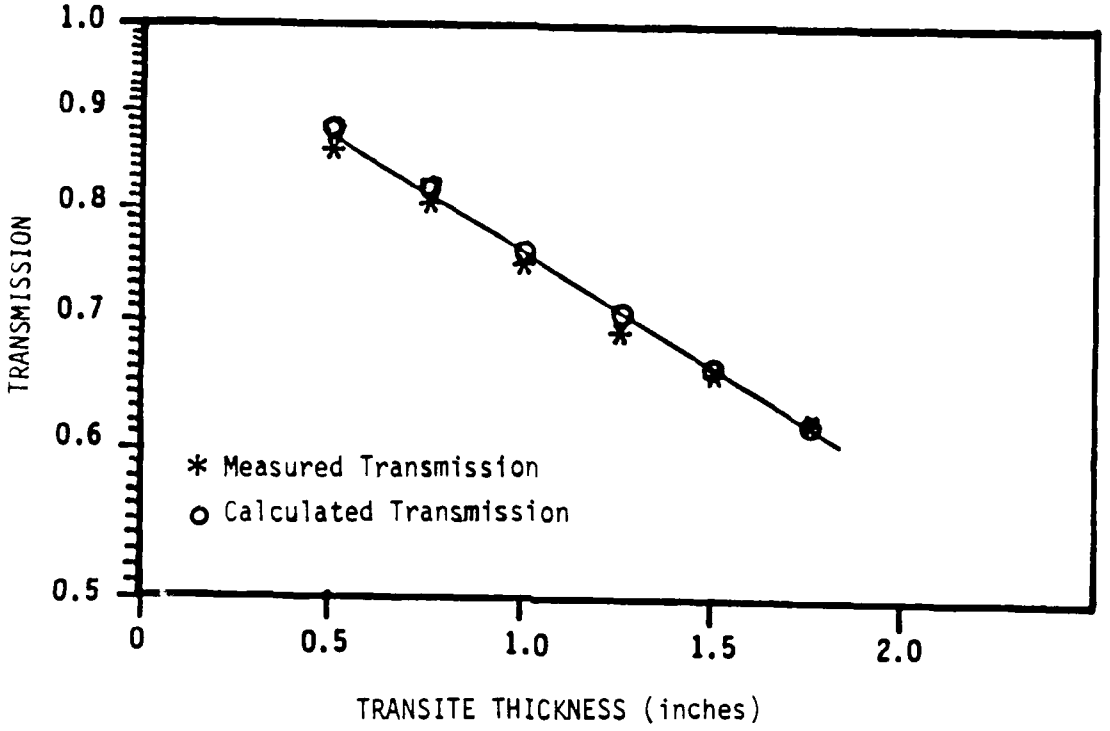

Figure 6. ^{60}Co (1.332 MeV γ) transmission in TRANSITE material.

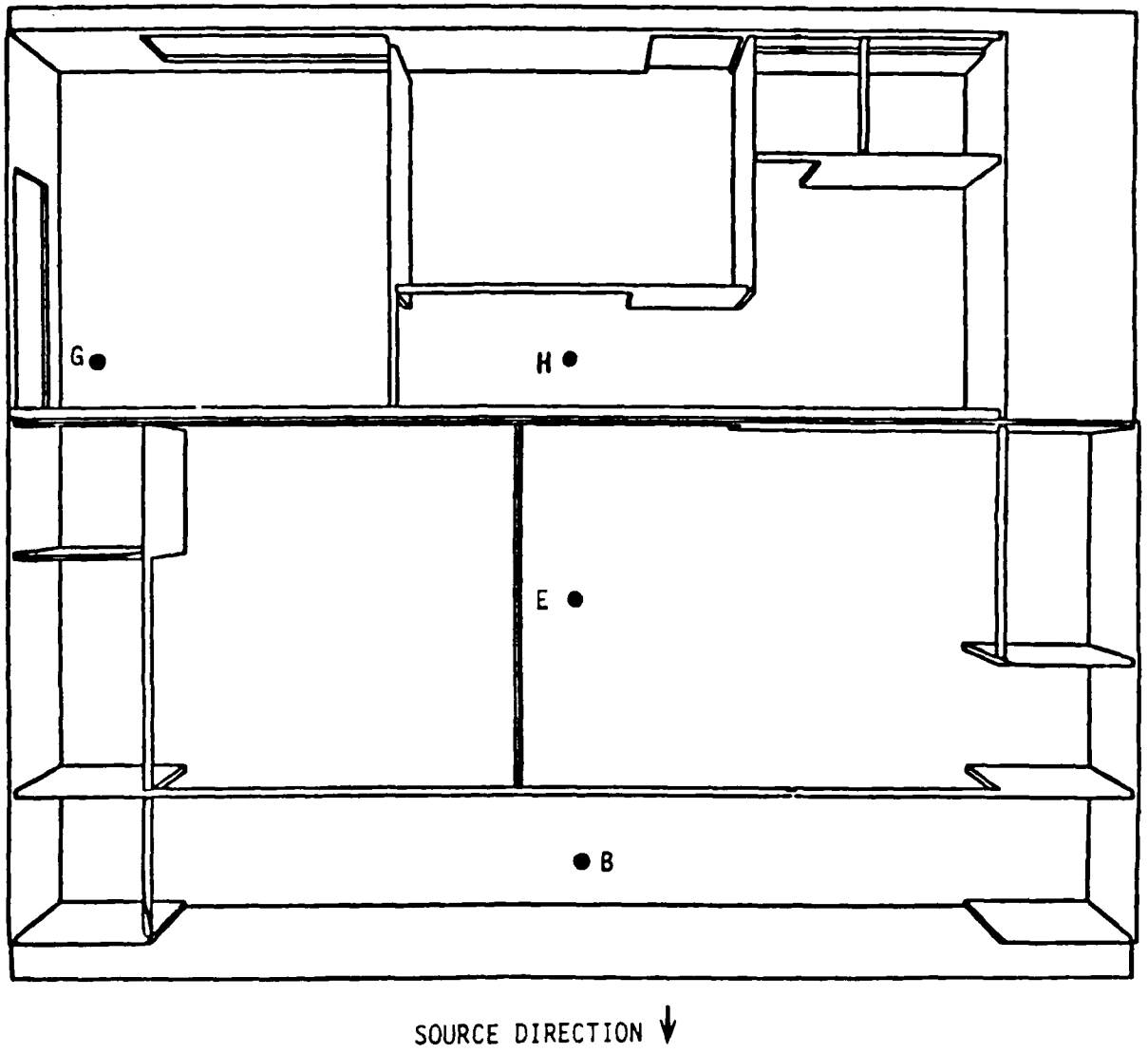

Figure 7. Interior of house A showing detector locations.

transmission factors for House A, for the ^{60}Co source and the HPRR source are presented in Table 3. For both measured and calculated, the transmission is the in-house kerma divided by the corresponding free field kerma. The HPRR gamma includes prompt gamma rays emitted from the reactor, secondary gamma rays produced in the air and ground and secondary gamma rays produced in the house materials. The comparison between the measured and calculated data for the ^{60}Co gamma-ray source is excellent. The neutron transmission factors are also in excellent agreement with the measured data. Since part of the calculational procedure involves the numerical calculation of the free-in-air environment, it is not possible to provide a computed estimate of the statistical uncertainty in the calculated results. However, the fractional standard deviations involved in the adjoint Monte Carlo calculation are all less than 5%.

The comparison of the calculated gamma-ray transmission from the HPRR source with the measured values, however, is not very good. At the two interior locations attempted, the calculated values are consistently lower than the measured data. The contributions to the gamma-ray transmission factor calculated are provided in Table 4. All values in the table are normalized to the FIA total calculated gamma-ray kerma. At the location of the house (750 yards ground range), approximately 75% of the free-in-air kerma comes from secondary gamma rays produced by the neutrons in the air and in the ground, and the other 25% are from the prompt gamma rays emitted from the reactor. The neutron kerma at this point is almost three times higher than the gamma-ray kerma. At the five-foot detector height for location E, our calculation of the gamma-ray kerma is nearly identical to the free-in-air gamma-ray kerma. In this instance, the gamma rays produced from neutron capture in the TRANSITE material offsets the attenuation of the incident gamma-ray kerma. A similar situation exists for the three-foot location H detector.

Table 3. Comparison of calculations with measurements of transmission factors for house A.

Location	Detector Height (ft)	^{60}Co Gamma		HPRR Neutron		HPRR Gamma	
		Measured	Calculated	Measured	Calculated	Measured	Calculated
B	3	0.62	0.63	----	----	----	----
E	3	0.56	0.55	0.48	0.48	----	----
E	5	0.40	0.41	0.46	0.44	1.44	1.02
G	5	----	----	0.48	0.44	----	----
H	3	0.40	0.44	0.41	0.43	1.32	0.97
H	5	----	----	0.43	0.38	----	----

Table 4. Gamma transmission analysis for house A and APRR source.

		Location H 3FT		Location E 5 Ft	
Component	FIA Kerma	Gamma TF	Gamma Kerma	Gamma TF	Gamma Kerma
Air/Ground Secondaries	0.744*	0.323	0.240	0.362	0.269
Prompt	0.256	0.441	0.113	0.488	0.125
Total Gamma	1.00	0.353	0.353	0.394	0.394
Neutron	2.90	0.214#	0.621	0.215#	0.624
	TOTAL CALCULATED		0.97		1.02
	MEASURED		1.32		1.44

*All values normalized to the calculated FIA total gamma-ray kerma.

#Multiples neutron FIA kerma to give gamma kerma fraction (e.g., 0.621 at location H, 3 ft) from secondary gamma-ray production in house materials.

Since the gamma-ray transmission factors for the prompt gamma rays and air secondary gamma rays appear reasonable, it was conjectured that the discrepancy between the calculated and measured values stems from the production of gamma rays in the house materials. To test this supposition, a one-dimensional spherical discrete ordinates calculation with the ANISN code[28] was performed for a shell source of the BREN HPRR neutron and gamma-ray spectrum at 750 yards ground range incident on spherical shells of varying TRANSITE thickness. The calculated gamma-ray transmission factor at the center of the sphere is given in Figure 8. The gamma transmission factor is a ratio of the gamma-ray kerma at the center of the sphere to the gamma-ray kerma at the shell source position. As the TRANSITE increases in thickness, the gamma-ray transmission factor increases because of the increased production of capture gamma rays. However, beyond a certain thickness, the self-shielding of these capture gamma rays in the TRANSITE reduces the transmission factor. The maximum transmission factor that we could calculate by this method was 1.2. The point on Figure 8 is plotted at the wall and roof thickness of TRANSITE for House A and indicates the transmission calculated by Monte Carlo for House A. The transmission is less than the spherical model, as expected, because the openings and rectangular geometry reduce the total capture source and transport to the detector. This indicates that it would be impossible to achieve transmission factors on the order of 1.4 with the cross sections used in our calculations because this spherical model maximizes the contribution from neutron induced gamma-rays. Since excellent agreement is obtained for the neutrons and ^{60}Co gamma-rays, the discrepancy does not lie in our geometry model of the house or the radiation transport procedure.

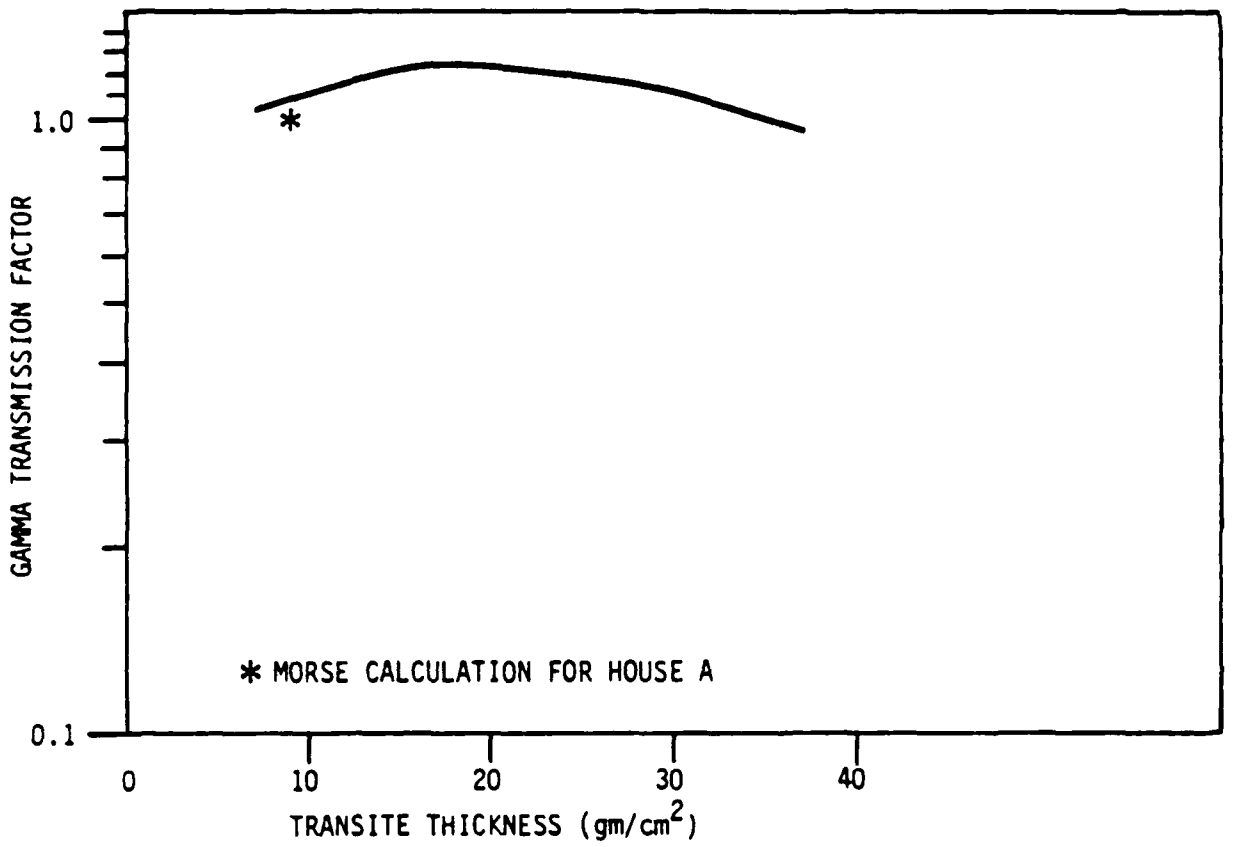

Figure 8. Maximum transmission factor model calculation for TRANSITE material.

It is possible that a strong secondary gamma-ray producer is present in the TRANSITE so that either the cross sections used in the computations for the given composition are in error, the large producer is among the elements detected but not incorporated into the calculations, or the large producer was not detected in the analysis of the TRANSITE samples. The elements not incorporated in the cross-section set for the calculations account for 0.04% of total mass (see Table 2). A bounding analysis of gamma production for these elements indicates they could not account for the 60% increase in the neutron to gamma transmission factor (see Table 4) required to produce agreement. By the same token, it is possible but not probable that the cause is due to cross-section errors or missing elements in the analysis.

Additional evidence indicates that the gamma-ray transmission measurements may be in error. We examined similar house transmission factor measurements made during the nuclear weapon explosions of Operation HARDTACK.[21] During operation HARDTACK, the House A TRANSITE houses were exposed to low yield nuclear weapons with a hard neutron output spectra similar to BREN and at source elevation angles similar to the BREN experiments. A comparison of results reported from the HARDTACK measurements with the BREN data is shown in Table 5. We also present our calculations for the BREN experiments. Note in Table 5 that the neutron transmission factors are reasonably consistent with one another, but that our calculations of the gamma transmission for BREN agree better with the HARDTACK data than the measured data at BREN. The gamma-ray measurements at HARDTACK were made with a chemical dosimeter system. In conjunction with the same anomalous high gamma-ray measurements in the FIA kerma,[23] we conclude at this time that the measured gamma-ray reported doses at BREN are probably in error due

Table 5. Comparison of transmission data for house A at BREN and HARDTACK.

	Neutron Transmission			Gamma Transmission		
Location	BREN Measured	BREN Calculated	HARDTACK Measured	BREN Measured	BREN Calculated	HARDTACK Measured
5' E	0.46	0.44	0.41	1.44	1.02	1.08
3' H	0.41	0.43	0.35	1.32	0.98	0.98

to either a calibration error or to neutron contamination of the Geiger detectors.

It is instructive to examine the in-house kerma as a function of the point of incidence of the external radiation field. This data can be invaluable devising generalized transmission factor models for application to Japanese A-bomb dosimetry. Tables 6 and 7 present the fraction of the exposure kerma according to its incidence on the large front opening. front and rear roof. "Front" and "rear" refer to directions facing toward and away from the source respectively and do not correspond in this case to what is normally called the "front" and "rear" of the house. For example, in Table 6, 0.2 x (FIA kerma) was detected at the 3 ft B location from radiation incident on the house through the front opening. The residual column tabulates kerma from incidence on the remaining house features. Data in Table 6 for the ^{60}Co indicate that for these detector locations the radiation through the front opening and front roof dominates the detected kerma. As one moves further back into the house the reduction in the transmission is caused by the reduction in the kerma from radiation incident on these house features. Similar conclusions can be made from the data exihibited in Table 7 for the neutron source. The higher fraction of dose from the residual components indicate the neutron environment is less forward peaked as expected.

Table 6. Fraction of total exposure kerma relative to FIA kerma from radiation incident on house components. For house A placed at 750 yards ground range and ^{60}Co source at height of 1125 ft.

Detector Location	Detector Height	House Component				Total Transmission
		Front Opening	Front Roof	Rear Roof	Residual	
B	3	0.20	0.36	0.003	0.067	0.63
E	3	0.18	0.30	0.01	0.06	0.55
E	5	0.10	0.22	0.01	0.08	0.41
H	3	0.11	0.22	0.03	0.08	0.44

Table 7. Fraction of total exposure neutron kerma relative to FIA neutron kerma from radiation incident on house component. For house A placed at 750 yards ground range and HPRR source at height of 1125 ft.

Detector Location	Detector Height	House Component				Total Transmission
		Front Opening	Front Roof	Rear Roof	Residual	
E	3	0.15	0.19	0.03	0.11	0.48
E	5	0.09	0.20	0.03	0.12	0.44
G	5	0.02	0.07	0.08	0.27*	0.44
H	3	0.08	0.14	0.08	0.13	0.43
H	5	0.05	0.13	0.08	0.12	0.38

*Of this residual 0.10 is due to radiation incident on an adjacent window.

5.4 CALCULATIONS FOR HOUSE B.

A model for a two story Japanese house used at BREN was called House B. Our rendition of House B used in the transport calculations is shown in Figures 9 and 10. We calculated transmission factors for the HPRR neutron and ^{60}Co sources at detector locations indicated in Figure 10. The comparison of our calculations with experimental data is given in Table 8. The source ground range and height was identical to those for House A. The source location column in Table 8 refers to the direction toward source referenced to the directions indicated in Figure 10. These comparisons show excellent agreement between calculation and measurement. The geometry of House B is considerably more complex than House A and the good agreement with some "difficult" detector locations indicates the ability of the transport calculations to adequately treat the effects of partitions, windows and multifloors.

5.5 CALCULATIONS FOR MULTIPLE HOUSE ARRANGEMENTS.

A high building density existed in typical residential neighborhoods of Hiroshima and Nagasaki ATB. In these built up areas with houses close tc another, the shielding effect of adjacent houses is important. To examine the multiple house shielding, the BREN experimenters placed the houses close together in a variety of arrangements and orientations with respect to the sources of radiation.

Two multiple house arrangements were calculated in our validation; one for ^{60}Co source and one for the HPRR neutron source. The BREN experimenters did not use an identical arrangement and orientation of House A and House B for both ^{60}Co and the HPRR. The two-house configuration using House

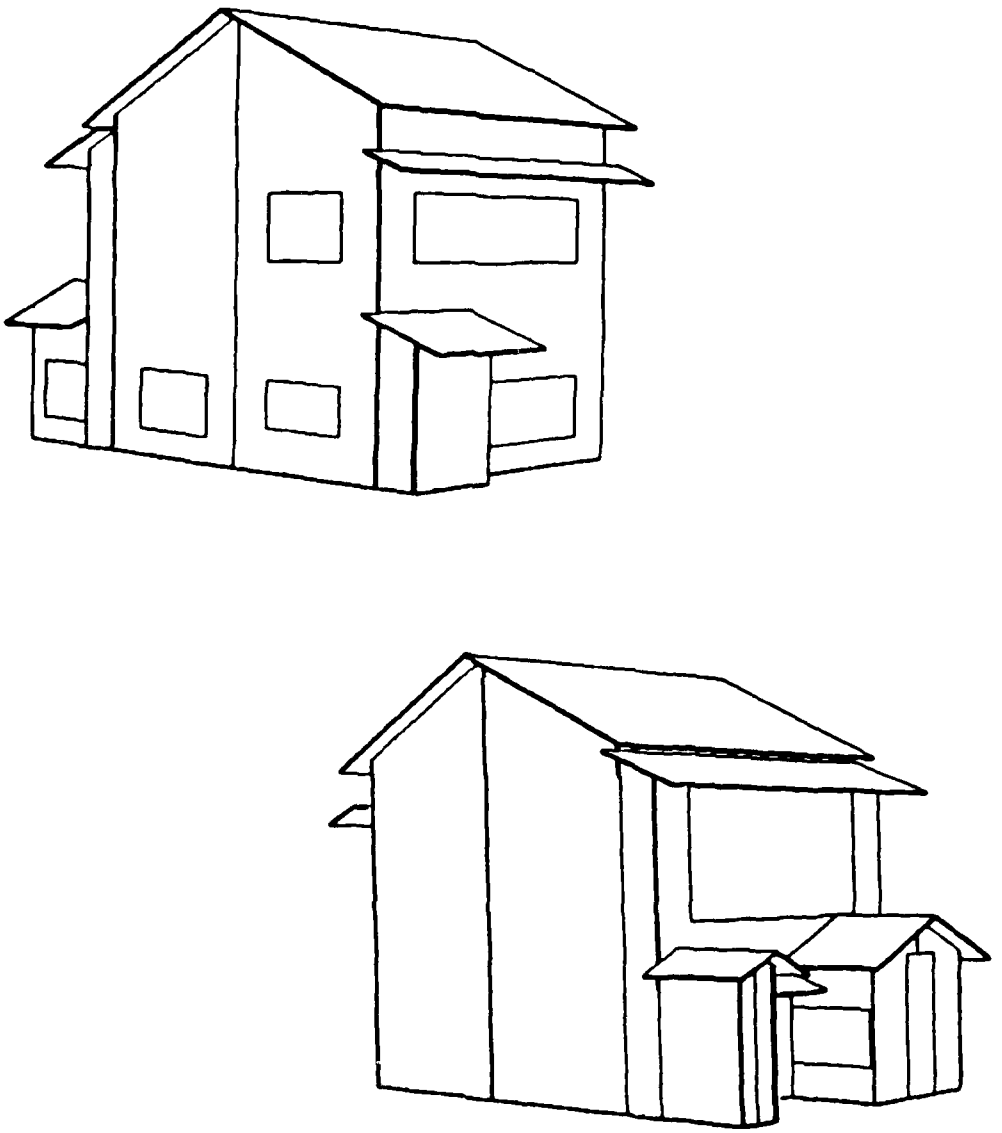

Figure 9. Geometry model of house type B.

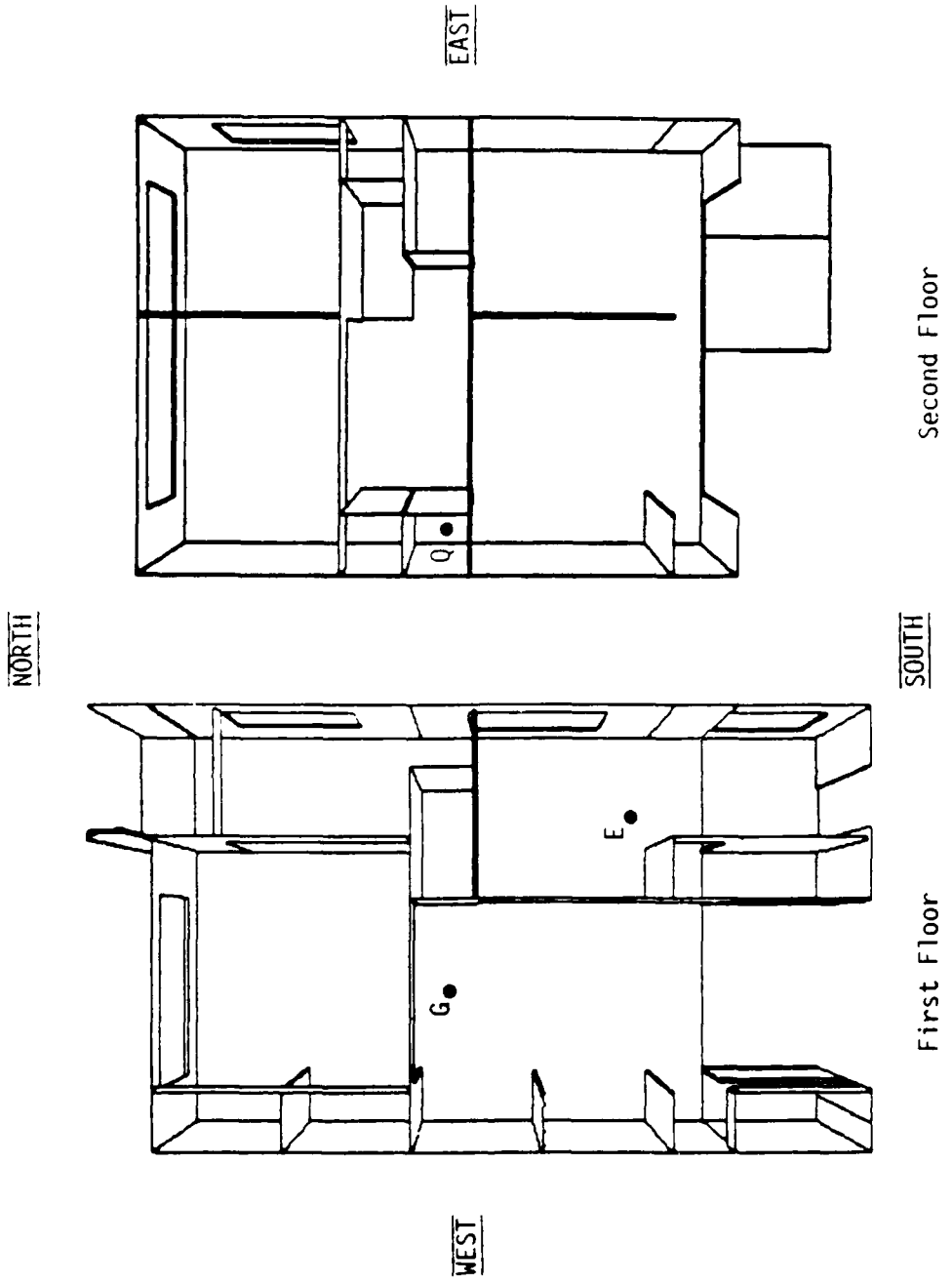

Figure 10. Interior of house B showing calculated detector locations.

Table 8. Comparison of calculations with measurements of transmission factors for house B.

Source Location	Detector Location	Detector Height (Off Floor)	^{60}Co Gamma		HPRR Neutron	
			Measured	Calculated	Measured	Calculated
South	G	5'	0.58	0.55	0.38	0.40
East	G	5'	0.29	0.26	----	----
South	E	3'	----	----	0.50	0.43
South	Q	5'	----	----	0.44	0.40

A and House B that we modeled for the ^{60}Co measurements is shown in Figure 11. In this configuration, the two-story House B shields the single story House A from the ^{60}Co source which was placed at the standard 750 yards ground range from the houses and at height of 1125 feet.

We compared calculations with experiment at three detector locations in House A. The results are given in Table 9. The agreement is very good. Also shown in Table 9 for comparison is our calculations of the transmission factor for House A without the intervening House B (reproduced from Table 3). This data indicates that House B in this configuration provides, roughly, the same amount of shielding as House A containing the detector.

The configuration used for the HPRR source is shown in Figure 12. Note that the arrangement of House A with respect to House B and the orientation of the source are different than the ^{60}Co source configuration. Three locations in House A and one location in House B were calculated and the results are provided in Table X. The agreement between calculation and experiment is excellent. A surprising result was the increase in transmission at location E with the addition of House B on the side. Evidently, House B acts as a scatter source of neutrons which increases the kerma in House A at location E. The situation is reversed for the 5' H location. Note, however, that for location H, House B blocks a large opening on the side and the mid-room partition shields scattered neutrons from the front portions of the side wall of House B. These results are not obvious <u>a priori</u>, but the agreement between experiment and calculation for both the single and multiple configuration confirms them.

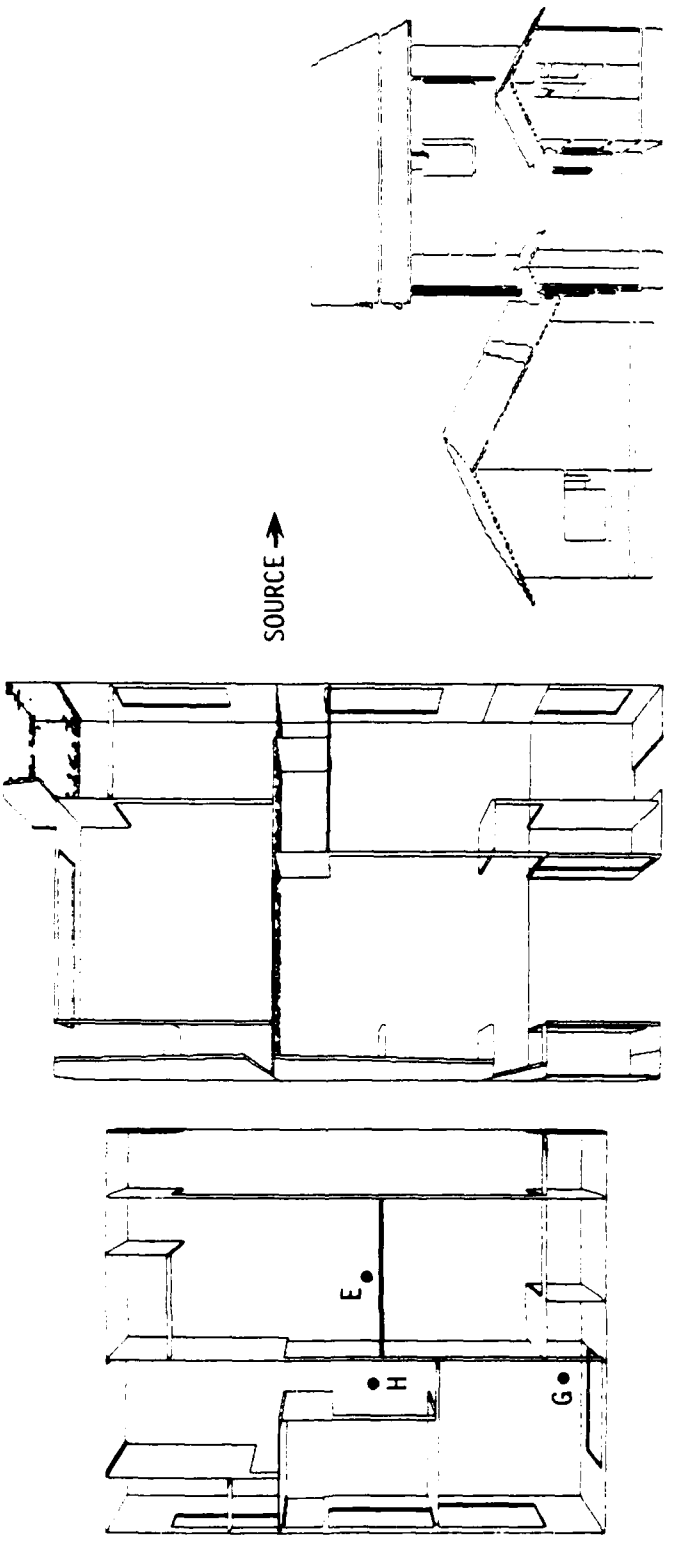

Figure 11. Multiple house configuration for ^{60}Co transmission factor calculations.

Table 9. Comparison of calculations with measurements of transmission factors for the ^{60}Co source in a multiple house configuration.

Detector Location	Detector Height	Multiple House Configuration		House A Standalone Calculated
		Measured	Calculated	
E	3'	0.16	0.18	0.48
H	3'	0.27	0.22	0.44
G	3'	0.16	0.18	----

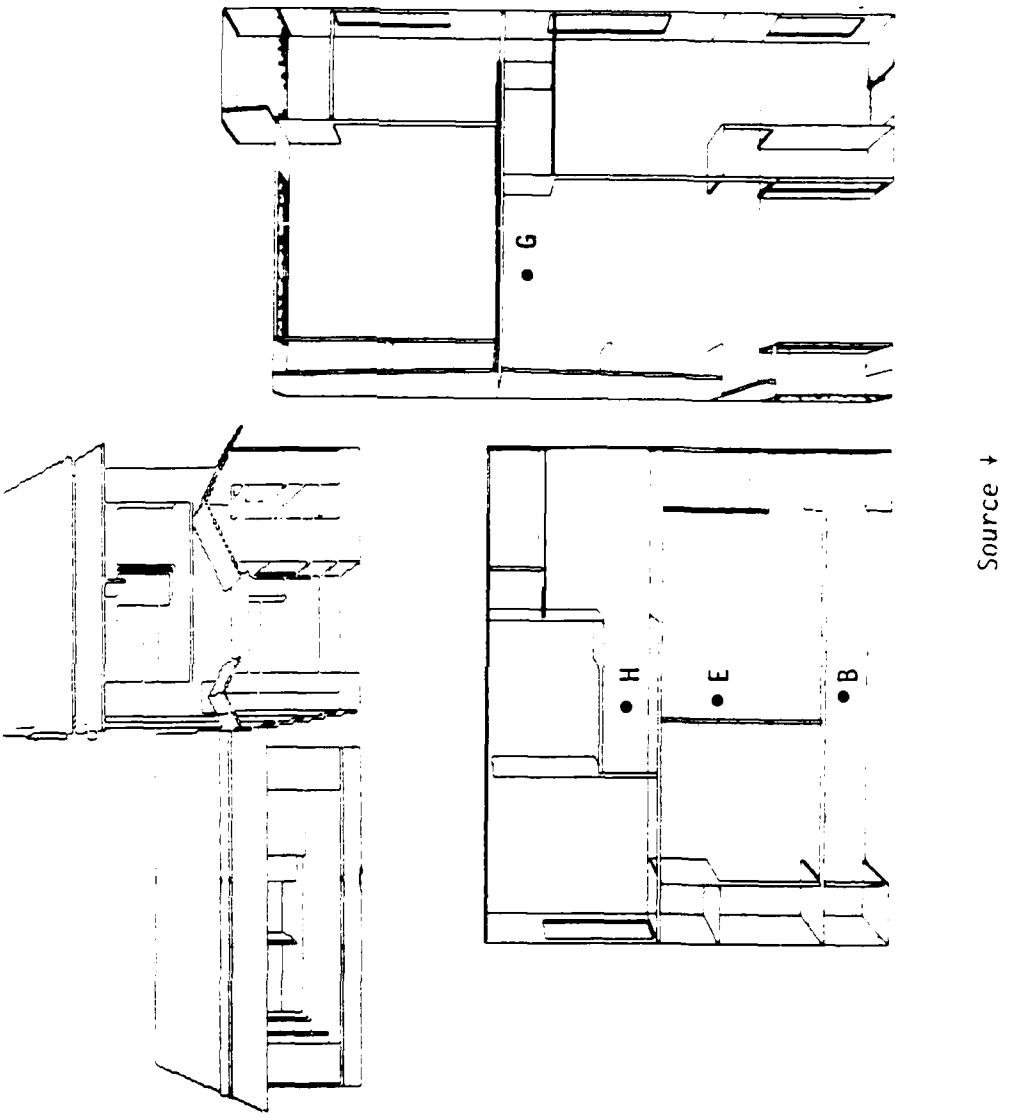

Figure 12. Multiple house configuration for HPRR transmission factor calculations.

Table 10. Comparison of calculations and measurements of neutron transmission factors for the HPRR source in a multiple house configuration.

Detection Location	Detector Height	Multiple House Configuration		House A Stand Alone Calculated
		Measured	Calculated	
B	3'	0.65	0.60	----
E	3'	0.60	0.60	0.48
H	5'	0.32	0.30	0.38
G*	3'	0.32	0.35	----

*Detector First Floor of House B

SECTION 6

CONCLUSIONS

The BREN house transmission experiments provide an excellent set of measurements to validate the calculational procedures that will be used to derive house shielding estimates for the revised dosimetry of the survivors of the Hiroshima and Nagasaki A-bombs. The BREN experiments were performed in realistic full scale models of Japanese residences. Although the radiation spectra and relative intensities of neutrons and gamma rays incident on the houses from the HPRR and the ^{60}Co sources are not appropriate for direct application to the A-bomb survivors, they cover the full energy range of importance. The codes and calculations required to compare with BREN experiments are the same as needed for the A-bomb dosimetry. They consist of a two-dimensional discrete ordinates calculation of the FIA environment coupled to an adjoint Monte Carlo calculation in detailed house geometry.

The agreement obtained between calculations and the experiments is excellent for neutrons and ^{60}Co gamma rays. Every house transmission calculation spanning simple to complex configurations and detector locations for the ^{60}Co and HPRR neutron cases was within an acceptable margin of error. The gamma-ray transmission calculations for the reactor source did not agree well with the experiments. Analysis of this discrepancy, however, strongly indicates that the problem probably does not reside in the calculational procedure, but in the measurements themselves.

In conclusion, we believe the excellent agreement of our calculations with the BREN experiments validates the calculational procedure we plan to apply to estimating the house shielding for survivors of the Hiroshima and Nagasaki A-bombs. Certainly, the calculations for Hiroshima and Nagasaki will involve modifications to the code used for the computations reported here, but to the extent that these modifications involve increased calculational complexity to treat more realistic materials and configurations, the benchmark established by these comparisons with the BREN experiments provides a valuable point of departure.

SECTION 7

LIST OF REFERENCES

1. "Reevaluations of Dosimetric Factors, Hiroshima and Nagasaki," Proceedings of a Symposium held at Germantown, Maryland, September 15-16, 1981, CONF-810928 (1982).
2. "US-Japan Joint Workshop for Reassessment of Atomic Bomb Radiation Dosimetry in Hiroshima and Nagasaki," Proceedings of a Workshop held at Nagasaki, Japan 16-17 February 1983.
3. J.A. AUXIER, "Ichiban: Radiation Dosimetry for the Survivors of the Bombings of Hiroshima and Nagasaki," ERDA Critical Review Series, TID-27080, NTIS (1977).
4. W.E. PREEG, Los Alamos Scientific Laboratory, letter to C.P. Knowles, R&D Associates (1976).
5. W.E. LOEWE and E. MENDELSOHN, "Neutron and Gamma Doses at Hiroshima and Nagasaki," UCRL-86596 Preprint, *Nuc. Sci. Eng.*, Vol. 81, No. 3 (1981).
6. J.S. CHEKA, F.W. SANDERS, T.D. JONES and W.H. SHINPAUGH, "Distribution of Weapons Radiation in Japanese Residential Structures," USAEC Report CEX-62.11, Oak Ridge National Laboratory, NTIS (1965).
7. W.A. WOOLSON, J. MARCUM, W.H. SCOTT, and V.E. STAGGS, "Building Transmission Factors," Proceedings of Symposium held at Germantown Maryland, CONF-810928 on September 15-16, 1981 (1982).
8. G.W. BEEBE and M. USAGAWA, "The Major ABCC Samples," TR 12-68, Atomic Bomb Casualty Commission (1968).
9. G.D. KERR, "Organ Dose Estimates for the Japanese Atomic-Bomb Survivors," *Health Phys.*, *37*, 487-508 (1979).
10. Calculation Method of Dose Received by Those Exposed Within Japanese Type Houses, Memorandum for Record, Field Operations Section, Hiroshima-Nagasaki, Atomic Bomb Casualty Commission (1964).

11. J. MARCUM, "House Attenuation Factors for Radiation at Hiroshima and Nagasaki," (Draft Report), unpublished R&D Associates (1981).

12. T.J. HOFFMAN, et al., *Nuc. Sci. Eng. 48*, 179 (1972).

13. W.A. RHOADES, "Development of a Code System for Determining Radiation Protection of Armored Vehicles (The VCS Code)," ORNL-TM-4664, Oak Ridge National Laboratory (1974).

14. M.L. GRITZNER, "A User's Manual for the Two-Dimensional Discrete Ordinate Code DOTSAI," SAI-75-747-HU, Science Applications, Inc. (1975).

15. E.A. STRAKER, W.H. SCOTT, JR., and N.R. BYRN,"The MORSE Code with Combinatorial Geometry," Report DNA-2860T, Defense Nuclear Agency (1972).

16. W.H. SCOTT, JR. and V.E. STAGGS,"Adjoint Energy Biasing and Thermal Neutron Diffusion in the MORSE and VCS Codes," Report SAI-133-81-384-LJ, Science Applications, Inc. (1981).

17. J.A. AUXIER, et al., "Technical Concept-Operation BREN," CEX-62.01, U.S. Atomic Energy Commission (1962).

18. J.A. AUXIER, *Health Physics, 11*, 89 (1965).

19. E.B. WAGNER and G.S. HURST, *Health Physics, 5*, 20 (1961).

20. G.S. HURST and E.B. WAGNER, *Rev. Sci. Instrum. 29*, 153 (1958).

21. J.A. AUXIER, J.S. CHEKA, and F.W. SANDERS, "Attenuation of Weapons Radiation: Application to Japanese Houses, Operation Hardtack," USAEC Report WT-1725, Oak Ridge National Laboratory, NTIS (1960).

22. Health Physics Division Annual Progress Report, USAEC Report ORNL-2806, 121-124, Oak Ridge National Laboratory (1959).

23. F. DOLATSHAHI and D.C. KAUL, "Calculations of Neutron and Gamma-Ray Transport in Air-Over-Ground Geometry -- Comparison with BREN and APR Experiments," Science Applications, Inc., to be published.

24. G. KERR, Private Communication from Intra-Laboratory Correspondence from J.F. Emery to George Kerr, (Jan. 19, 1983).

25. R.W. ROUSSIN, et al., "PVC-36 Group, P_5, Photon Interaction Cross Sections for 38 Materials in ANISN Format," DLC-48, Oak Ridge National Laboratory (1977).

26. D.E. BARTINE, et al., "Production of Testing of DNA Few-Group Coupled Neutron-Gamma Cross-Section Library," ORNL-4840, Oak Ridge, National Laboratory (1977).

27. D. SHREVE, Private Communication (1983).

28. W.W. ENGLE, JR., "A User's Manual for ANISN," K-1693, Oak Ridge National Laboratory (1967).

DISTRIBUTION LIST

DEPARTMENT OF DEFENSE

ARMED FORCES RADIOBIOLOGY RSCH INST
ATTN: RBD
ATTN: RSD
ATTN: TECHNICAL LIBRARY

ASSISTANT TO THE SECRETARY OF DEFENSE
ATOMIC ENERGY
ATTN: EXECUTIVE ASSISTANT

DEFENSE INTELLIGENCE AGENCY
ATTN: DB
ATTN: DB-4, RSCH RESOURCES DIV
ATTN: DT
ATTN: DT(SCI-TECH INTELL)
ATTN: RTS-2B

DEFENSE NUCLEAR AGENCY
ATTN: DFRA
ATTN: NANF
ATTN: OPNA
2 CYS ATTN: RARP
4 CYS ATTN: TITL

DEFENSE TECHNICAL INFORMATION CENTER
12CYS ATTN: DD

FIELD COMMAND DEFENSE NUCLEAR AGENCY
ATTN: FCPR
3 CYS ATTN: FCPRT
ATTN: FCTXE
ATTN: FTTD W SUMMA
ATTN: NUC SECURITY

INTERSERVICE NUCLEAR WEAPONS SCHOOL
ATTN: TTV
2 CYS ATTN: TTV 3416TH TTSQ

LAWRENCE LIVERMORE NATIONAL LABORATORY
ATTN: DNA-LL

DEPARTMENT OF THE ARMY

U S ARMY BALLISTIC RESEARCH LAB
ATTN: AMXBR-VLD-R, DR RAINIS
ATTN: AMXBR-VLD, DR KLOPCIC
ATTN: DRDAR-BL
ATTN: DRDAR-BLA-S, TECH LIB
ATTN: DRDAR-BLT

U S ARMY NUCLEAR & CHEMICAL AGENCY
ATTN: DR DAVIDSON
ATTN: LIBRARY

DEPARTMENT OF THE AIR FORCE

AIR FORCE WEAPONS LABORATORY
ATTN: SUL

DEPARTMENT OF ENERGY

DEPARTMENT OF ENERGY
ATTN: OMA, DP-22

LAWRENCE LIVERMORE NATIONAL LAB
ATTN: D DIVISION
ATTN: L-53 TECH INFO DEPT LIB
ATTN: Z DIVISION LIBRARY

LOS ALAMOS NATIONAL LABORATORY
ATTN: REPORT LIBRARY
ATTN: T DOWLER
ATTN: R SANDOVAL

SANDIA NATIONAL LABORATORIES
ATTN: TECH LIB 3141/RPTS REC CLK
ATTN: 0333 R B STRATTON
ATTN: 0334 J STRUVE

OTHER GOVERNMENT

FEDERAL EMERGENCY MANAGEMENT AGENCY
ATTN: ASST ASSOC DIR FOR RSCH
ATTN: CIVIL SECURITY DIV
ATTN: G ORRELL NP-CP
ATTN: OFC OF RSCH/NP H TOVEY

U S NUCLEAR REGULATORY COMMISSION
ATTN: DIR DIV OF SAFEGUARDS
ATTN: S YANIV

US DEPARTMENT OF STATE
ATTN: PM/STM

DEPARTMENT OF DEFENSE CONTRACTORS

ADVANCED RESEARCH & APPLICATIONS CORP
ATTN: DOCUMENT CONTROL

KAMAN SCIENCES CORP
ATTN: E CONRAD

KAMAN SCIENCES CORPORATION
ATTN: DASIAC

KAMAN TEMPO
ATTN: DASIAC

PACIFIC-SIERRA RESEARCH CORP
2 CYS ATTN: G ANNO
ATTN: H BRODE, CHAIRMAN SAGE

PACIFIC-SIERRA RESEARCH CORP
ATTN: D GORMLEY
2 CYS ATTN: G MCCLELLAN

R & D ASSOCIATES
ATTN: C MCDONALD
2 CYS ATTN: DOCUMENT CONTROL
ATTN: F A FIELD

R & D ASSOCIATES
ATTN: A DEVERILL
ATTN: C KNOWLES
ATTN: J THOMPSON
ATTN: K MORAN
ATTN: W GRAHAM

SCIENCE APPLICATIONS INTL CORP
ATTN: DOCUMENT CONTROL
ATTN: E SWICK
ATTN: J MARTIN
ATTN: J WARNER
ATTN: M DRAKE
2 CYS ATTN: M GRITZNER
ATTN: R J BEYSTER

SCIENCE APPLICATIONS INTL CORP
ATTN: B BENNETT
ATTN: D KAUL
ATTN: DOCUMENT CONTROL
ATTN: J FOSTER
ATTN: J PETERS
ATTN: J SHANNON
ATTN: L GOURE
ATTN: M FINEBURG
ATTN: W LAYSON
ATTN: W SCOTT
2 CYS ATTN: W WOOLSON

SCIENCE APPLICATIONS INTL CORP
ATTN: R CRAVER

END

DATE

FILMED

6-88

DTIC